HAW HAMBURG

Master Thesis

Basic Comparison of Three Aircraft Concepts: Classic Jet Propulsion, Turbo-Electric Propulsion and Turbo-Hydraulic Propulsion

Author: Clinton Rodrigo

Supervisor: Prof. Dr.-Ing. Dieter Scholz, MSME

Submitted: 2019-09-22

Faculty of Engineering and Computer Science
Department of Automotive and Aeronautical Engineering

DOI:
https://doi.org/10.15488/9329

URN:
https://nbn-resolving.org/urn:nbn:de:gbv:18302-aero2019-09-22.014

Associated URLs:
https://nbn-resolving.org/html/urn:nbn:de:gbv:18302-aero2019-09-22.014

Any further request may be directed to:
Prof. Dr.-Ing. Dieter Scholz, MSME
E-Mail see: http://www.ProfScholz.de

This work is part of:
Digital Library - Projects & Theses - Prof. Dr. Scholz
http://library.ProfScholz.de

Published by
Aircraft Design and Systems Group (AERO)
Department of Automotive and Aeronautical Engineering
Hamburg University of Applied Science

This report is deposited and archived:

- Deutsche Nationalbiliothek (https://www.dnb.de)
- Repositorium der Leibniz Universität Hannover (https://www.repo.uni-hannover.de)
- Internet Archive (https://archive.org)
  Item: https://archive.org/details/TextRodrigo.pdf

This report has associated published data in Harvard Dataverse:
https://doi.org/10.7910/DVN/K5FLHR

Abstract

Purpose – This paper presents a comparison of aircraft design concepts to identify the superior propulsion system model among turbo-hydraulic, turbo-electric and classic jet propulsion with respect to Direct Operating Costs (DOC), environmental impact and fuel burn.
Approach – A simple aircraft model was designed based on the Top-Level Aircraft Requirements of Airbus A320 passenger aircraft, and novel engine concepts were integrated to establish new models. Numerous types of propulsion system configurations were created by varying the type of gas turbine engine and number of propulsors.
Findings – After an elaborate comparison of the aforementioned concepts, the all turbo-hydraulic propulsion system is found to be superior to the all turbo-electric propulsion system. A new propulsion system concept was developed by combining the thrust of a turbofan engine and utilizing the power produced by the turbo-hydraulic propulsion system that is delivered via propellers. The new partial turbo-hydraulic propulsion concept in which 20% of the total cruise power is coming from the (hydraulic driven) propellers is even more efficient than an all turbo-hydraulic concept in terms of DOC, environmental impact and fuel burn.
Research Limitations – The aircraft were modelled with a spreadsheet based on handbook methods and relevant statistics. The investigation was done only for one type of reference aircraft and one route. A detailed analysis with a greater number of reference aircraft and types of routes could lead to other results.
Practical Implications – With the provided spreadsheet, the DOC and environmental impact can be approximated for any commercial reference aircraft combined with the aforementioned propulsion system concepts.
Social Implications – Based on the results of this thesis, the public will be able to discuss the demerits of otherwise highly lauded electric propulsion concepts.
Value – To evaluate the viability of the hydraulic propulsion systems for passenger aircraft using simple mass models and aircraft design concept.

Keywords: aeronautics, airplanes, aircraft, aircraft design, flight mechanics, aircraft performance, engines, turbofan engines, electric propulsion, hybrid propulsion, distributed propulsion, hydraulics, certification, evaluation, DOC, environment, Airbus, A320

Table of Contents

Page

List of Figures

List of Tables

List of Symbols

$\dot{m}$	Flow Rate
A	Aspect Ratio
a	Slope
a	Speed of Sound
B	Breguet Range Factor
C	Coefficient
C	Costs
d	Diameter
D	Drag
E	Glide Ratio
e	Oswald Efficiency Factor
g	Acceleration due to Gravity
h	Altitude
k	Factor
L	Disc Loading
L	Labor Rate
l	Length of Pipe
L	Lift
M	Mach Number
m	mass
M	Mass Fraction
n	Drive Speed of the Motor and Pump
n	Number
p	Operating Pressure
P	Rated Power
Q	Volumetric Flow
R	Range
S	Area
S	Maximum Allowable Stress
T	Temperature
t	Thickness
T	Thrust
t	Time
TE	Turbo-Electric
TH	Turbo-Hydraulic
V	Velocity
W	Weight

Greek Symbols

Δ	Absolute Roughness Coefficient
γ	Climb Angle
λ	Darcy Friction Factor
ρ	Density
κ	Dimensionless Coefficient
ν	Displacement
ν	Dynamic Viscosity
η	Efficiency
π	Pi – Mathematical Constant
σ	Relative Density
Δ	Difference

Indices

$()_{APP}$	Approach
$()_{cable}$	Cable
$()_{cor}$	Correction
$()_{CR}$	Cruise
$()_{D}$	Drag
$()_{D,P}$	Profile Drag
$()_{DEP}$	Depreciation
$()_{DES}$	Decent
$()_{E}$	Engine
$()_{em}$	Electric Motor
$()_{EPS}$	Electric Propulsion System
$()_{ET}$	Entry Temperature
$()_{f}$	Fluid
$()_{f}$	Fuel
$()_{F}$	Fuel
$()_{FEE}$	Fees
$()_{ff}$	Fuel Fraction
$()_{flow}$	Flow
$()_{fus}$	Fuselage
$()_{gen}$	Generator
$()_{H}$	Horizontal Tail plane
$()_{hm}$	Hydraulic Motor
$()_{hp}$	Hydraulic Pump

$()_{in}$	Inner
$()_{INT}$	Interest
$()_{L}$	Landing
$()_{L}$	Lift
$()_{LFL}$	Landing Field Length
$()_{LOI}$	Loiter
$()_{M}$	Maintenance
$()_{M}$	Motor
$()_{max}$	Maximum
$()_{md}$	Minimum Drag
$()_{ML}$	Maximum Landing
$()_{MTO}$	Maximum Take-off
$()_{new}$	New
$()_{o}$	Outer
$()_{OE}$	Operating Empty
$()_{P}$	Propeller
$()_{PAX}$	Passengers
$()_{pe}$	Power Electronics
$()_{pipe}$	Pipe
$()_{PO}$	Power Output
$()_{pp}$	Pressure Pipe
$()_{RES}$	Reserve
$()_{rp}$	Return Pipe
$()_{s,\ TO}$	Sea-level, Take-off
$()_{s,1}$	Stall Speed
$()_{STD}$	Standard
$()_{SYS}$	Systems
$()_{TO}$	Take-off
$()_{TOFL}$	Take-off Field Length
$()_{TP}$	Turboprop
$()_{TS}$	Turboshaft
$()_{V}$	Vertical Tail plane
$()_{W}$	Wing
$()_{wet}$	Wetted Area

List of Abbreviations

A320	Airbus 320
ACARE	Advisory Council of Aeronautics Research in Europe
AEA	Association of European Airlines
AERO	Aircraft Design and Systems Group
BDL	Bundesverband Der Deutschen Luftverkehrswirtschaft
BLI	Boundary Layer Ingestion
BPR	Bypass Ratio
CFD	Computational Fluid Dynamics
DOC	Direct Operating Costs
EASA	European Union Aviation Safety Agency
EI	Environmental Impact
EPNdB	Noise Level in Effective Perceived Noise in Decibels
EPS	Electric Propulsion System
GT	Gas Turbine
HAW	Hochschule für Angewandte Wissenshaften
HPS	Hydraulic Propulsion System
ICAO	International Civil Aviation Organization
LCA	Life Cycle Assessment
MTOW	Maximum Take-Off Weight
NAS	National Academies of Sciences
NASA	National Aeronautics and Space Administration
OEM	Original Equipment Manufacturer
OPerA	Optimization in Preliminary Aircraft Design
OPR	Overall Pressure Ratio
PreSTo	Preliminary Sizing Tool
PSFC	Power Specific Fuel Consumption
SRIA	Strategic Research and Innovative Agenda
SS	Single Score
SS	Stainless Steel
TLAR	Top-Level Aircraft Requirements
TSFC	Thrust Specific Fuel Consumption

List of Definitions

The definitions provided below are defined according to Gunston (2009) unless specified.

Emissions	A substance discharged into the air, as by an internal combustion engine (Crocker 2011).
Direct Operating Cost	Costs of operating transport aircraft, usually expressed in pence or cents per seat-mile, per US ton-mile or per mile, and including crew costs, fuel and oil, insurance, maintenance and depreciation.
Hybrid Propulsion	Aircraft propelled by two or more dissimilar species of prime mover.
Life Cycle	Essentially self-explanatory, the sequence of phases through which a product may be expected to pass.
Turboprop	Gas turbine similar to turbofan but with extra turbine power geared down to drive propeller.
Turboshaft	Gas turbine for delivering shaft power to power helicopter.
Turbofan	Comprises of gas-turbine core engine, essentially a simple turbojet, plus extra turbine stages driving large-diameter fan ducting very large propulsive airflow round core engine and generating most of thrust.
Range	The maximum distance an aircraft can fly on a given amount of fuel (Crocker 2011).
Specific Fuel Consumption	Rate of consumption of fuel for unit power or thrust, and thus basic measure of efficiency of prime mover.

1 Introduction

1.1 Motivation

Air travel plays a crucial role in today's world. Every aircraft manufacturing company continuously try to improve their design and efficiency. Aviation regulators on the other hand tend to lay promising regulations for the future to cut down the carbon emissions and to promote a greener environment. Also, limitation of petroleum resources is a major driver for research in green energy. Besides emissions, the industry is also looking for ways to reduce the cost of air travel in order to encourage more people to fly.

A hybrid propulsion system concept is being used in most of the vehicles today to cut down the same carbon emissions. Many OEMs have already started adapting the hybrid concept in aviation like the Airbus E-fan X. By combining the classic jet propulsion and electric propulsion, one can achieve at least a few of the above-mentioned goals.

Hydraulic propulsion systems are widely used in the Marine industry and are also the mechanical back-bone of an aircraft. But a hydraulic propulsion system was never investigated for aviation purpose even though they have significant mass advantage over the electrical systems. Among the three propulsion systems, the storage of aviation fuel is the best option in terms of specific power. In order to overcome this complication., a hybrid of electric/hydraulic and jet propulsion can be determined to reduce the overall fuel consumption. For this reason, Prof. Scholz from the AERO group in Hamburg University of Applied Sciences wanted to evaluate the conventional propulsion system along with two new concepts.

1.2 Title Terminology

The terms used in the thesis title are defined below. The definitions are defined according to Gunston (2009) unless specified.

Aircraft Device designed to sustain itself in atmosphere above Earth's surface, to which it may be attached by tether that offers no support.

Concept An idea or abstract principle (Crocker 2011).

Jet Propulsion Aircraft propulsion by any propulsion system whose reaction is generated by a jet, thus a turbofan, turbojet or ramjet.

Propulsion An act or instance of pushing or driving forward (Crocker 2011).

Turbo	A generalized prefix meaning driven by or associated with gas turbine engine.
Hydraulic System	Complete aircraft installation comprising closed circuits of piping, engine-driven pumps, accumulators, valves, heat exchangers and filters.
Electric	Powered or worked by electricity (Crocker 2011).

1.3 Objectives

The main objective of this thesis is to find the superior propulsion system concept for passenger aircraft with respect to Direct Operating Costs and environmental impact. To study in detail the various propulsion concepts. To model a turbo-hydraulic and turbo-electric propulsion system. The propulsion system concept considered for comparison are turbo-electric, turbo-hydraulic and classic jet propulsion. Also, to evaluate a range of hybrid concepts developed by combining different gas turbine engines.

1.4 Previous Research

This thesis is mainly a continuation of research by Prof. Scholz who has studied various concepts of aircraft design and has evaluated the electric and hybrid concepts. The aircraft design concept represented in this thesis was according to Scholz (2018a). It is part of the lecture of aircraft design course at HAW Hamburg. The course consists of all the essential knowledge required to make a preliminary aircraft design sizing. It also includes a section for Direct Operating Costs (DOC), where the topic is well explained and consists all the statistical values required.

Although the concept of turbo-hydraulic propulsion was not studied before, a preliminary study was done in Scholz (2018b) which was the starting point of this research. For the basic formulae required to design a hydraulic system, Hatami (2019) and NPTEL (2013) was used.

The turbo-electric concept has been researched by various manufacturers and researchers for a while. But the initial information and explanation about various electric propulsion concepts were provided by Scholz (2018b) and NAS (2016). The NAS (2016) **c**onsisted of the basic definitions and comparison of the all the electric propulsion concepts. Gesell (2017) and Aigner (2018) also helped in the basic working principle of the concept. There are many papers regarding this subject published by NASA and two of them that were helpful are Welstead 2016 and Felder 2011.

For the Life Cycle Assessment of the aircraft, there are various concepts available to use. Johanning (2016) served as a compilation all such concepts with a well-designed tool. Since the A320 aircraft was used a reference aircraft, a lot of basic parameters of the aircraft was required. These values were mostly extracted from Nita (2013) and Airbus (2019).

1.5 Structure of the Work

The structure of this thesis is explained below

Chapter 2 It gives an overview of existing research of all the propulsion concepts along with their basic working principle. It also includes the advantages and disadvantages of the concepts.

Chapter 3 This chapter covers the sizing method of turboprop, turboshaft, hydraulic and electric propulsion system. It mainly includes the mass estimations and architecture of the systems. It of consists of existing and newly developed empirical models.

Chapter 4 The preliminary sizing for the aircraft concepts are explained briefly here. The calculation of direct of costs and life cycle assessment of the aircraft is also determined.

Chapter 5 This section covers the results of the calculation done. The results are represented in tables and graphs. The results are also briefly discussed, and reasoning is given.

Chapter 6 Conclusion and summary of all the concepts are provided here. The best concept chosen.

2 Literature Review

2.1 Classic Jet Propulsion

According to different conditions, a distinct type of jet engine exists. A difference is made in a number of design characteristics such as compressors, distribution of airflow with the engine and the number of spools.

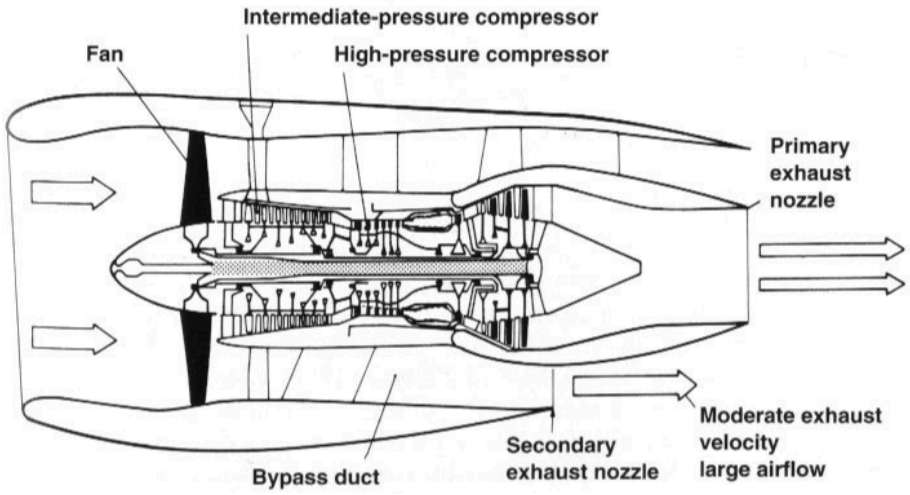

Figure 2.1 Turbofan engine schematic (Hünecke 2003)

The earliest type of gas turbine propulsion was the turbojet. The simple design consisted of a compressor, combustor and a turbine. Because of the technological progress, the turbofan engine has become the most common type of engine in commercial aviation aircraft. The turbofan engine is a turbojet engine installed with a fan with a large diameter. This fan is driven by the low-pressure turbine which is designed to absorb from the hot gas than required. Only a part of the air enters the core engine after passing through the fan. The remaining air is bypassed and expands in the nozzle to provide thrust. The ratio of the air bypassed to the air entering the core engine is known as the bypass ratio.

The fuel consumption of the aircraft is greatly improved due to high bypass ratio turbofan engines. The important advantage of turbofan engine is that it produces high level of thrust during take-off. Also, it is proven to be relatively quieter than other engines. The CFM 56 series engine used in the A320 produces a thrust of 120 kN and has a bypass ratio of 6:1 (Hünecke 2003). However, the turbofan engines consume kerosene, and which is not a green fuel. Therefore, alternate fuels and propulsions systems are being researched and demonstrated. They are presented in the following chapters.

2.2 Electric Propulsion

Over the last decade, electric propulsion models have been be continuously researched and optimized to provide the rapidly growing aviation market with ecologically efficient propulsion systems. The crucial goals of this research have been on reducing the fuel burn, emissions and noise. Some examples of the research initiatives are Strategic Research and Innovative Agenda (SRIA) by the Advisory Council of Aeronautics Research in Europe and the NASA N+3 goals. The aim of the SRIA is to achieve a 75% improvement in energy efficiencies by the year 2050 compared to the baseline year of 2000 (ACARE 2012). The electric propulsion can be sub-divided into three main types and they are:

- All electric propulsion
- Hybrid Propulsion
- Turbo-electric propulsion

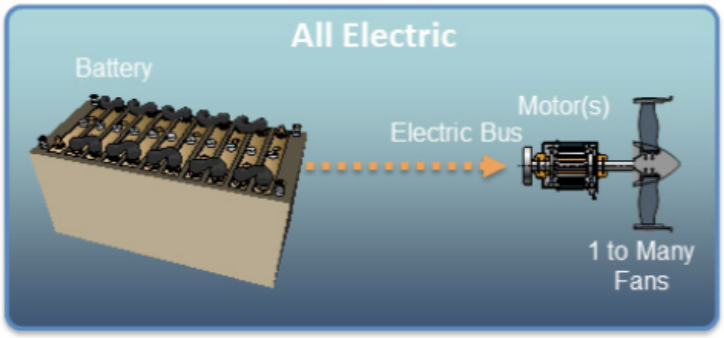

Figure 2.2 All electric propulsion architecture (NAS 2016)

The all-electric propulsion system uses the batteries located in the aircraft as the only source of power. It is a simple principle where the chemical energy of the batteries is converted into mechanical energy that drives the motor. The advantages gained with the all-electric propulsion is that it has almost zero local emissions. It is also known to reduce noise pollution of the aircraft while flying and on ground. However, the mass of fuel that is the battery is very high compared to the Jet fuels. The limitations are mainly due to relatively less energy density and power density. Therefore, they can only power small aircraft efficiently (Aigner 2018).

A recent advancement in the all-electric aircraft market was the Airbus E-fan. This aircraft was developed to demonstrate the electric propulsion technology in the aviation market and also cater to the pilot training industry. After identifying the viability in hybrid propulsion, Airbus cancelled the current project and pivoted towards creating the E-Fan X concept in order to increase the power output (Rapoport 2017).

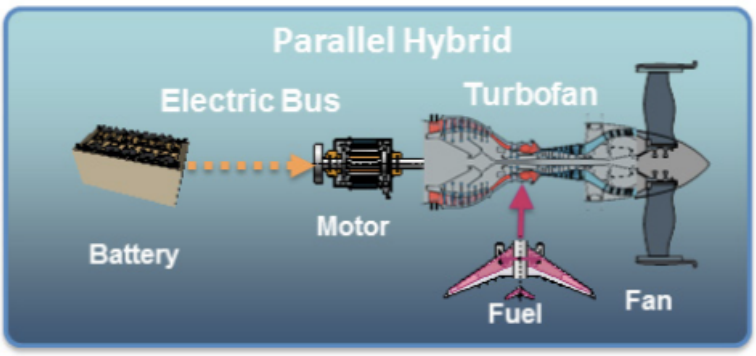

Figure 2.3 Hybrid electric propulsion architecture (NAS 2016)

Unlike the all-electric propulsion system, the hybrid electric propulsion concept derives energy from two sources, the Gas turbine engine (GT) and a battery. In this propulsion system, the energy is distributed optimally during different phases (take-off, climb, cruise, and decent) of the flight. Power density can be a limitation in this propulsion system. The degree of hybridization should be well planned to take into consideration of take-off and climb operating points.

The two types of hybridization are hybrid-electric serial and hybrid-electric parallel. In hybrid- electric parallel model, the electric motor is mounted on the shaft of the GT engine as shown in Figure 2.3. The hybrid-electric serial model the electric motor and GT are decoupled (Gesell 2018).

2.3 Hydraulic Propulsion

A hydraulic system can be defined as a system that produces high magnitude of controlled force. This force is produced by pressurizing incompressible liquids as a transmission media. The hydraulic system contains the ability to produce large force using a small force input. The theory behind the production of this large force is derived from Pascal's law which says that "the pressure in an enclosed fluid is uniform in all directions". The main applications of hydraulic systems are industrial machineries, mobile hydraulic equipments, braking systems in automobiles, propulsion system in marine applications and as system components in aviation.

In aviation, the hydraulic system is used in landing gear system, braking system and control surfaces. The hydraulic system is used widely due to its high efficiency and the potential to deliver power consistently which the other mechanical drive systems lack of. A typical hydraulic system consists of pump, reservoir, control valve, movable piston, pressure regulator leak-proof piping (NPTEL 2013).

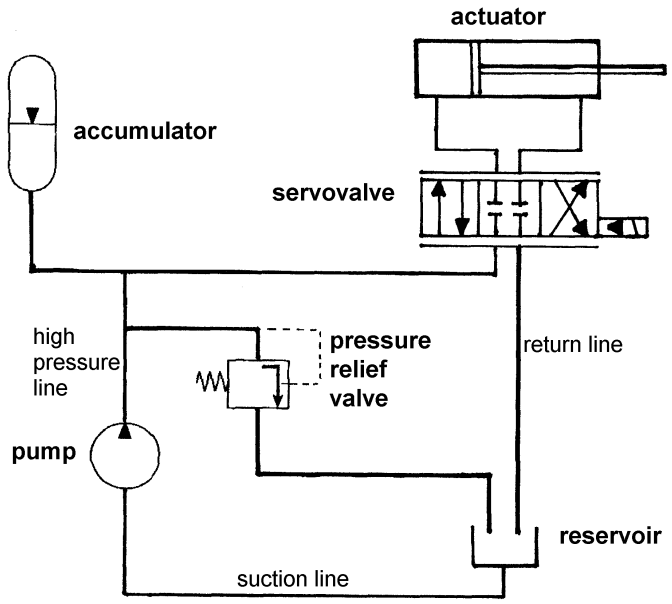

Figure 2.4 A basic hydraulic system (Scholz 2019)

Using a suction line, the pump draws fluid from the reservoir and increases the pressure to the required level. Typically for transport aircraft, the pressure level is 3000 psi or 5000 psi. The fluid is pressure is scrutinized by the pressure relief valve and automatically dissipates excess pressure by drawing it back to the reservoir. The accumulator acts as an energy storage device. A control valve determines the motion of the actuator piston which leads to the movement of a control surface (Scholz 2019). In Figure 2.9, the actuator is replaced by a motor for this research.

2.4 Turbo-Hydraulic/Electric Propulsion

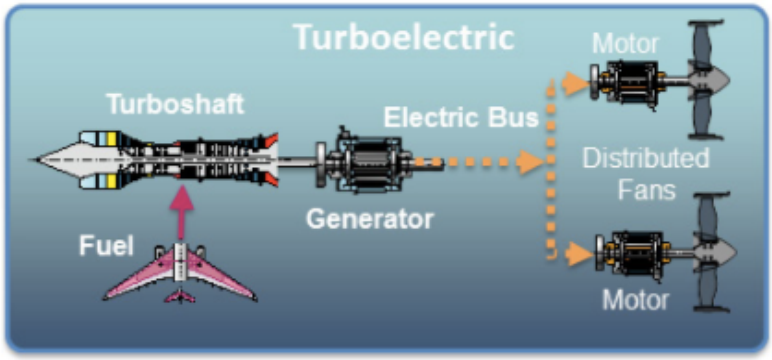

Figure 2.5 Turbo-electric propulsion architecture

The turbo-electric concept eliminates the need for a battery. In this case, the source of power generation and the propulsor are decoupled. By doing this, the speeds and inlet-to-outlet ratios are also decoupled. The benefit is extracted from high BPR, since many fans can be powered by one single turbine. This in turn improves the propulsive efficiency of the system. Since the fan and turbine are decoupled, the speed ratios can be set and varied during the operation. It also allows the fan to be placed at an optimum location in the aircraft since the transmission of power is electrical. The process of placing propulsors close to the body of the aircraft and reenergizing the boundary layer is known as Boundary Layer Ingestion (BLI). This helps in reducing the drag since the slow-moving flow is ingested, accelerated and exhausted.

Figure 2.6 Bauhaus luftfahrt's concept aircraft with aft propulsor (Warwick 2018)

The Bauhaus luftfahrt's aircraft in Figure 2.6 demonstrates the BLI with a propulsor in the aft of the aircraft. This third engine provides about 23% of the total thrust. This turbine engine ingests the airflow and reenergizes the momentum deficit that is caused by the profile drag and skin friction (Warwick 2018).

Table 2.1 List of turboelectric aircraft with their requirements

Model Name	Number of Passengers	Max. Power (MW)	Range (NM)
NASA STARC-ABL (Welstead 2017)	154	2.6	3500
NASA N3-X (Felder 2011)	300	50	7500
Wright ECO-150R (Schiltgen 2016)	150	12.7	1650

Table 2.1 contains the list of aircraft that are currently being researched to be launched in the next decades with turboelectric aircraft. The two NASA aircraft use the state-of-the-art super-conductive electric drives that is still under research. The concept is to use superconductive materials for motors, generators and cables that are almost 100% efficient and have high specific power. The ECO-150R has teamed with the airline EasyJet to build a short-range small aircraft with conventional electric engines which is targeted to be enter service in 2035.

Similar to the Turbo-electric propulsion, the Turbo-hydraulic propulsion system generates power using the Gas turbine engine. This power is used to drive the hydraulic pump. The hydraulic fluid is then pressurized by the pump and then flows through the pressure pipe to drive the hydraulic motor which is equipped with a propeller as shown in Figure 2.7. Unlike the turbo-electric propulsion, there are no previous research completed on this topic.

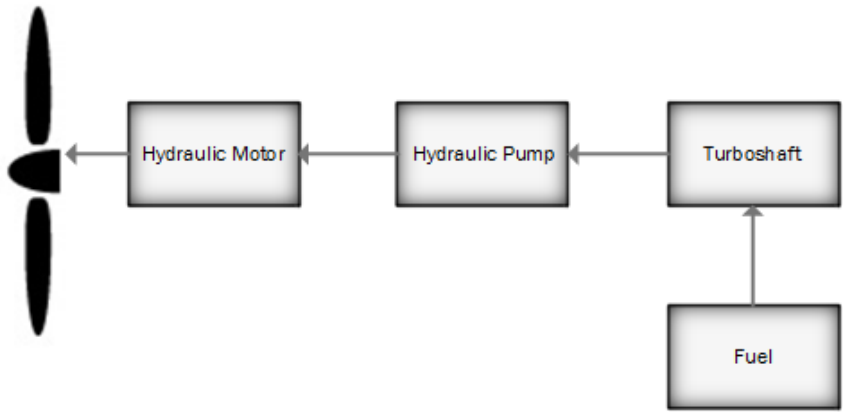

Figure 2.7 Turbo-hydraulic propulsion architecture

In Scholz 2018b, a concept for a hybrid concept was brought into light. For this concept, the overall efficiency of the system depends on the pump, motor, propeller and piping. While designing such a system one must make sure the components used are flight proven. This is because a hydraulic system is typically not used in an aircraft that utilizes power of this magnitude.

3 Sizing Methodology of Propulsion Systems

This chapter explains in detail the sizing methods of all the propulsion systems used. Especially, the hydraulic propulsion is explained in detail because of lack of previous research. The electric propulsion system is sized by using existing models and empirical data. There are two types of gas turbine engines (turboshaft and turboprop) that are used for turbo-hydraulic/electric models. The term motor is used to describe electric or hydraulic motor, depending on the context.

3.1 Hydraulic Propulsion System

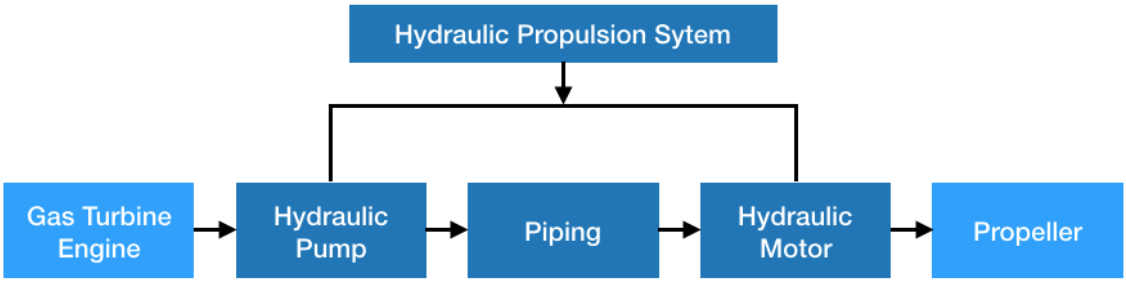

Figure 3.1 Turbo-hydraulic Propulsion System Architecture

The utilization of a Hydraulic system in aircraft propulsion is a novel concept. Although, they have been propelling ships and boats for quite a while. Since hydraulic systems are used for other sub-systems in an aircraft, it benefits one in the requirements for an airborne technology. For this reason, the system components sizing of the Hydraulic Propulsion System (HPS) will be derived from flight rated components available in the industry. The methodology for sizing HPS is taken from various sources.

In order to size a hydraulic system, the basic parameters of such a system must be defined. This includes defining Operating pressure (p), rated power (P), Volumetric flow (Q), drive speed of the motor and pump (n) and displacement (v). The only known parameter would be the output power required and this will be derived in the following chapters. p and n can be determined by inputting various values for them and narrowing down to a realistic value. The formulae used for hydraulic pump and motor are taken from the Rexroth Formulary by Hatami (2013). It is assumed that the hydraulic pump is attached to the shaft of a Gas Turbine (GT) engine and that the output power of the GT is the input power of hydraulic pump.

$$P_{PO} = \frac{p \cdot Q}{600 \cdot \eta_{pump}} \tag{3.1}$$

In the Equation (3.1), P_{PO} stands for power output of the pump in kW. Q is measured in l/min and p in bar. P_{PO} and p are known while η_{pump} is assumed to be 0.9. By modifying the equation to solve for Q, we obtain the following.

$$Q = \frac{P_{PO} \cdot 600 \cdot \eta_{pump}}{p} \tag{3.2}$$

Using Q and rpm (n), the displacement (v) can be determined but rpm is unknown. Therefore, by inputting values from 1000 to 14000 for n one can identify the ideal value by applying the following equation. The ideal value can be identified by comparing all the parameters of the pump with an existing pump in the industry.

$$v = \frac{60 \cdot 1.66 \cdot 10^{-1} \cdot Q}{n} \tag{3.3}$$

The working of the pump is now defined. The next step is to size the pipe diameter of the piping between the pump and motor. As mentioned previously, for simplicity, only pump, piping and motors are considered. The sizing of the pipe diameter is done according to Parker (2013).

$$d_i = 4.61 \cdot \left(\frac{Q}{V_{flow}}\right)^{0.5} \tag{3.4}$$

The Equation 3.4 can be used to find the minimum inner diameter (d_i) of the pipe. It depends on Q and velocity of the flow (V_{flow}). According to Scholz (1998), the average fluid velocity for an Airbus aircraft is 10 to 12 m/s for pressure lines and 6-8 m/s for return lines. In order to determine the thickness of the pipe (t), the outer diameter (d_o) must be a known value.

$$p = S \cdot \frac{(d_o^2 - d_i^2)}{(d_o^2 + d_i^2)} \tag{3.5}$$

$$d_o^2 = d_i^2 \cdot \frac{\left(\frac{p}{S} + 1\right)}{\left(1 - \frac{p}{S}\right)} \tag{3.6}$$

(3.5) is used to determine operating pressure but one can one can remodel the equation to (3.6) to find the outer diameter. In this equation the diameters must be inputted in inches and the pressure in psi. S is the maximum allowable stress for a specific material. For this research, Stainless Steel 304 is chosen due to its high S of 18,800 psi. There is a pressure drop across the pipe and this pressure is denoted by Δp. Δp can be determined using the Darcy-Weisbach equation given below (Kudela 2010).

$$\Delta p = \lambda \cdot \frac{l}{d_i} \cdot \frac{V_{flow}^2}{2} \cdot \rho_f \tag{3.7}$$

λ	Darcy friction factor, see below
l	length of the pipe (m)
ρ_f	density of the hydraulic fluid (kg/m^3)

$$\lambda = 0.11 \cdot \left(\kappa + \frac{68}{Re}\right)^{0.25} \tag{3.8}$$

$$\kappa = \frac{\Delta}{d_i} \tag{3.9}$$

$$Re = \frac{V_{flow} \cdot d_i}{\nu} \tag{3.10}$$

The pressure loss can be found using (3.7) along with (3.8), (3.9) and (3.10). Δ is the absolute roughness coefficient of the pipe material which is approximately 0.00015 mm for Stainless Steel 304 and ν in (3.10) is the dynamic viscosity of the hydraulic fluid. The hydraulic fluid chosen for this research is Skydrol. Skydrol is a flight-proven hydraulic fluid used in the aviation industry by many aircraft. The dynamic viscosity and density of Skydrol are 0.00001249 m^2/s and 1000 kg/m^3 (Skydrol 2003).

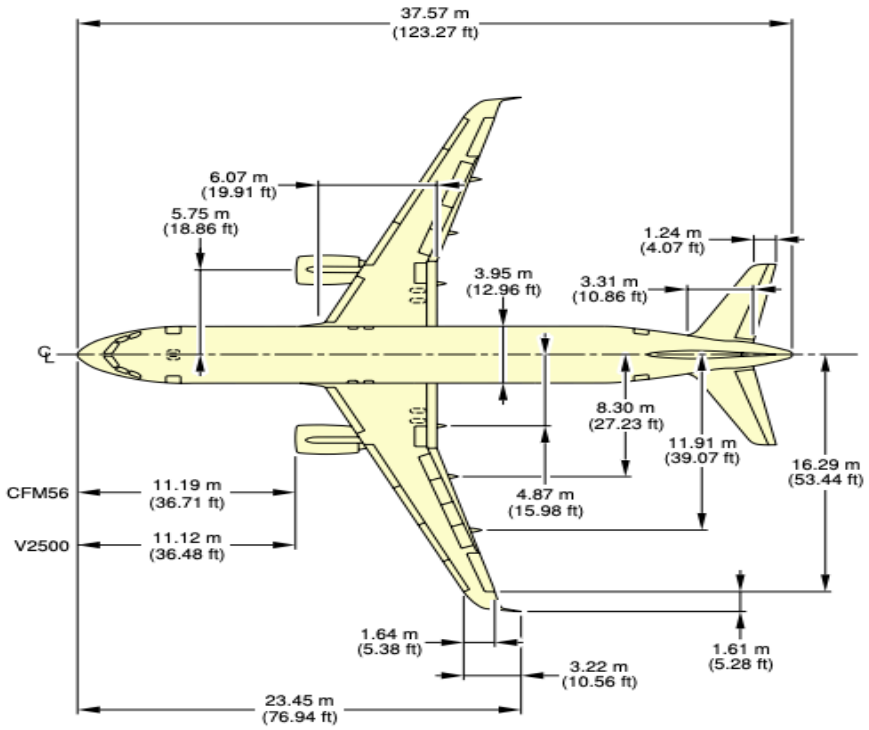

Figure 3.2 Dimensions of Airbus 320 aircraft (Airbus 2005)

The length of the piping depends mainly on the location of the pump and the motor. Initially, the gas turbine engine and the pump were placed in the aft of the aircraft. This reduced the noise and insulation required while acting as an optimum position for exhaust. But since the piping required is long, it led to a significant increase in mass of piping and reduction in efficiency. To overcome this effect, the gas turbine engine and hydraulic pump were placed in the centre under-belly of the aircraft as shown in Figure 3.1. The exact dimensions required were measured from Figure 3.2.

Since there is a pressure drop, a new pressure (p_{new}) is obtained. This can be calculated subtracting the pressure difference (Δp) from standard operating pressure (p). The efficiency of the pipe can be defined.

$$\eta_{pipe} = 1 - \frac{\Delta p}{p} \tag{3.11}$$

Subsequentially, the parameters of the motor are obtained. This can be done in a method similar to the pump. The new pressure must be utilized to calculate the parameters. The same efficiency is used for pump and motor and the value is 0.9.

To proceed further in the sizing of the HPS, one must identify the mass of the defined components. Since the size of the motor and pump depend mainly on the required power by the aircraft, therefore a standard motor available from the industry cannot be used. The mass of the pump, motor and the piping are mainly considered.

$$m_{pp} = l \cdot \rho_p \cdot \left(\frac{\pi d_o^2}{4} - \frac{\pi d_i^2}{4}\right) \tag{3.12}$$

$$m_f = l \cdot \rho_f \cdot \frac{\pi d_i^2}{4} \tag{3.13}$$

$$m_{pipe} = m_{pp} + m_{rp} + m_f \tag{3.14}$$

Using (3.12) and (3.13) the mass of the pressure line pipe (m_{pp}) and mass of fluid (m_f) can be calculated. The density of SS 304 material is said to be 7888 kg/m^3 (Peckner 1977). According the return line is calculated by multiplying the mass of the pressure by 60%. This is a safe approximation since the pressure in the return line pipe is very low. Therefore, the total mass of the pipe m_{pipe} can be determined by using (3.14). The total mass of the pipe is strangely heavy due to the high magnitude flow rate. Therefore, considering that it can be optimized with the technological advancement in the future, the mass of the pipe is reduced by 50%. Now, one can find an optimum operating pressure for the system. This can be done by plotting all the pressure values against the total mass of the pipe and fluid.

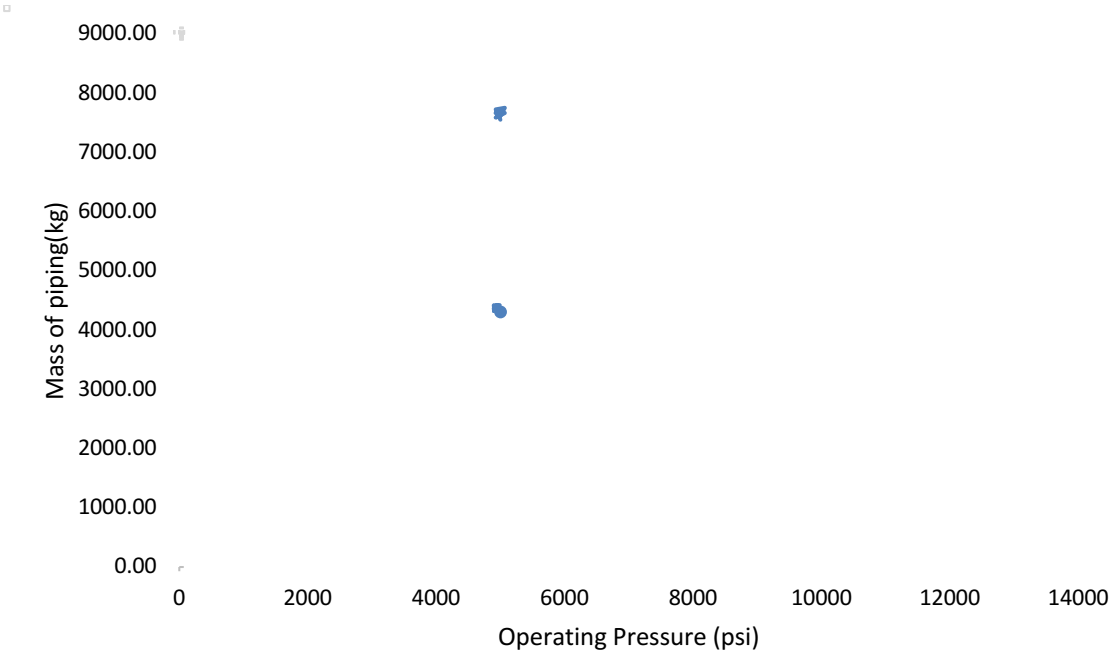

Figure 3.3 Operating pressure vs. Mass of the hydraulic piping

The graph provides a clearer vision about the relation between operating pressure and the mass of the piping. The increase in pressure decreases the flow rate of the fluid. This in turn decreases the internal diameter of the pipes and therefore reducing the mass of the required fluid. However, the increase in pressure increases the thickness of the pipe and thus increasing the mass.

The mass of the piping is sum of the mass of the pipes and the fluid. Therefore, provides an optimum pressure of 5000 psi. It is clear from the graph that lower pressure reduces the mass. But one cannot use an operating pressure less than 5000 psi because it hikes the rpm (n) and displacement (v) for the required magnitude of power. To have a rational approach pressure below 5000 psi are avoided. Another reason for this opting for this pressure is because latest aircraft have a hydraulic system with 5000 psi. Therefore, it helps in combining the HPS with the local hydraulic system.

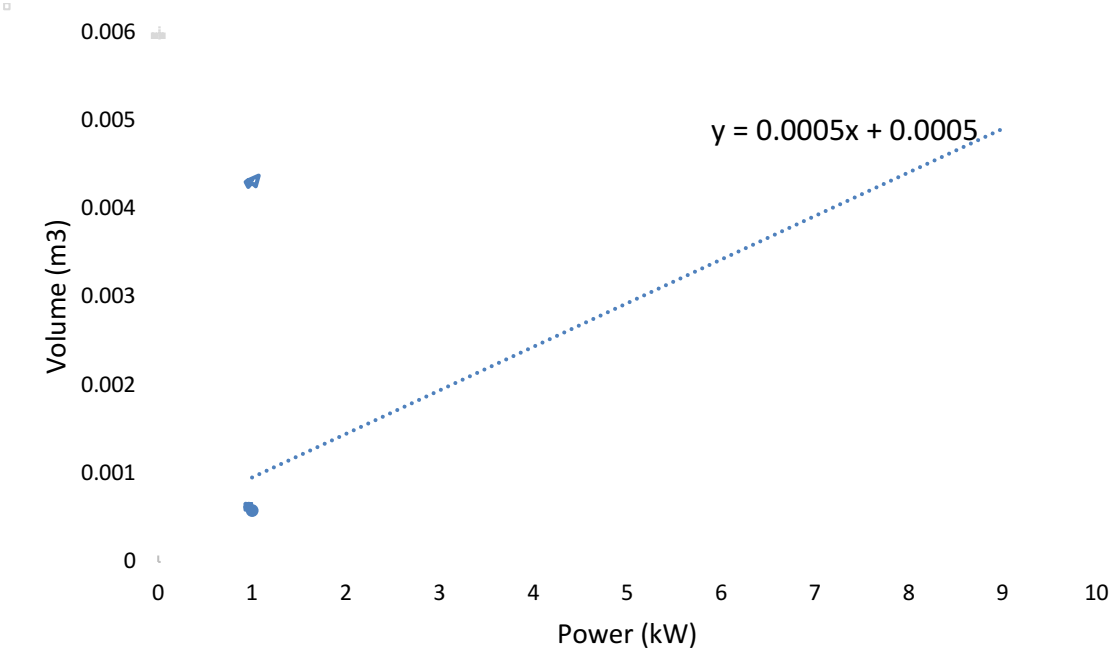

Figure 3.4 Hydraulic pump/motor volume statistic

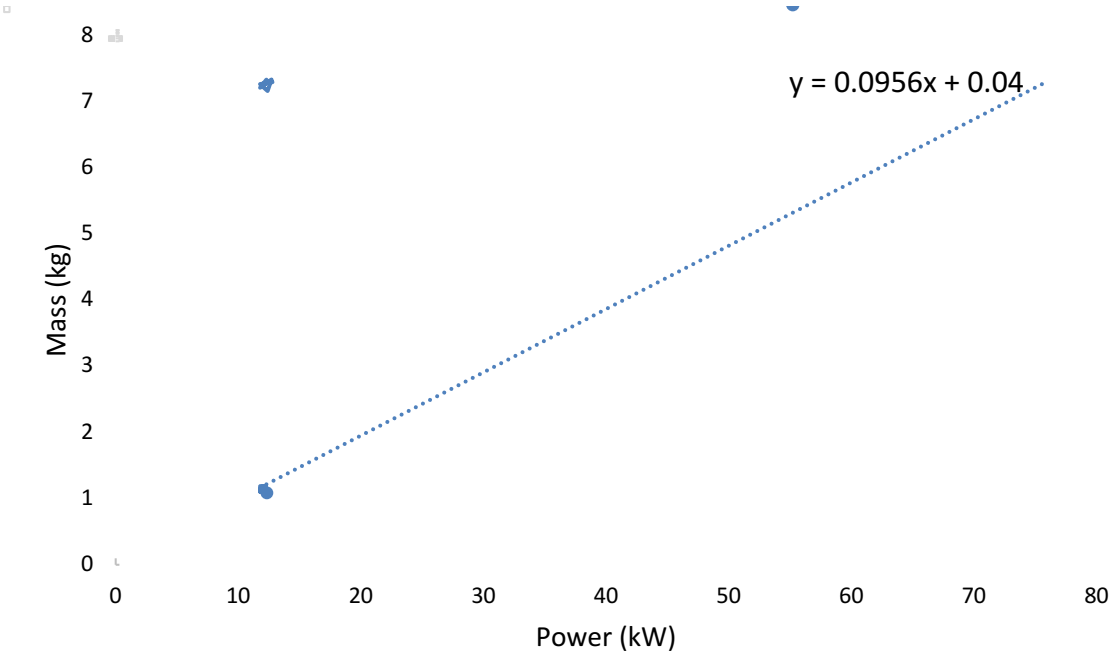

Figure 3.5 Hydraulic pump/motor mass statistic

Data from the product sheet of Parker (2009) to plot a graph with power produced against mass of the pump. These pumps are used as engine-driven pumps in various aircraft to supply hydraulic power with the variable displacement axial piston pump system. In the product sheet, the parameters such as flow rate and operating pressure were provided for more than 20 pumps. From Figure 3.4, one can calculate the volume of a pump or a motor whenever required during the aircraft design process. From the Figure 3.5, the power-to-weight ratio for a hydraulic pump/motor can be deduced as 10 kW/kg.

Table 3.1 Hydraulic pump/motor statistic

Model of hydraulic pump	**Specific Power**
Parker Hannifin	10 kW/kg
Hydroeluc M12	11 kW/kg
Hydroeluc M18	16.7 kW/kg
Average	12.8 kW/kg

In Table 3.1, two additional models of hydraulic pumps are described. They are Digital Displacement hydraulic pumps according to Caldwell (2018). This pump is equipped with a radial piston machine that is controlled by computer-controlled valves. The benefits of this new technology as opposed to the analog machines are improved efficiency, reduced losses and high precision. Thus, now by averaging the specific power there is a new value of 12.8 kW/kg.

$$m_{hp} = 12.8 \cdot P \tag{3.15}$$

$$m_{HPS} = m_{hp} + m_{pipe} + m_{hm} \tag{3.16}$$

$$\eta_{HPS} = \eta_{hp} \cdot \eta_{pipe} \cdot \eta_{hm} \sim 77\% \tag{3.17}$$

$()_{hp}$ hydraulic pump

$()_{hm}$ hydraulic motor

To conclude the sizing of the HPS, (3.15), (3.16) and (3.17) can be used to identify the overall mass and efficiency of the hydraulic propulsion system.

3.2 Electric Propulsion System

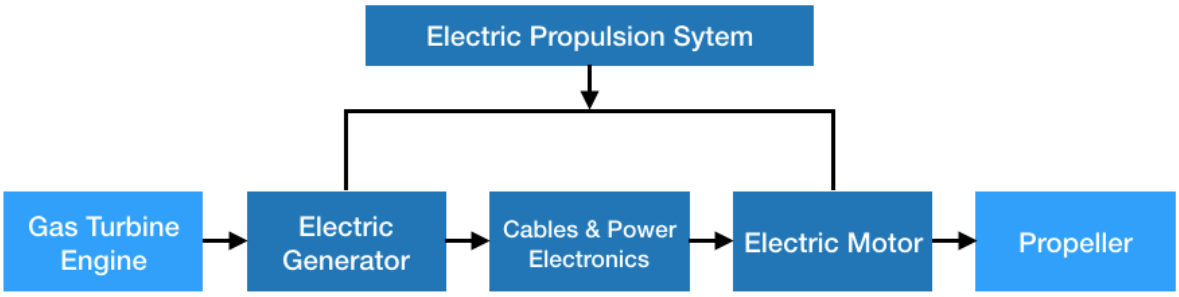

Figure 3.6 Turbo-electric propulsion system architecture

Similar to HPS, the electric propulsion system (EPS) will have the same architecture with electric components as seen in Figure 3.6. The basic requirements for an EPS are components such as generators, motors and cables. Unlike HPS, the EPS have been utilized numerous times in recent days. This provides us with diverse data to summarize in order to acquire the mass of EPS.

Table 3.2 Electric motor/generator statistic

Model Name	Efficiency	Specific Power (kW/kg)
Siemens (Anton 2018)	94%	5.9
NASA HW FEP (Rosario 2014)	-	6.6
Gesell (2018)	95%	7.35
Compact Dynamics (2016)	90%	6.5
Average	93%	6.58

In Table 3.2, parameters of electric motor/generator from different sources are presented. The Siemens motor was used for the experimental electric aircraft manufactured by Diamond aircraft. The NASA motor is part of a Fixed Wing Hybrid Electric Propulsion technology roadmap that aims to achieve a specific power of 20 kW/kg by 2030. The third source is from a science journal, where a description of present electric propulsion technology is evaluated. In this journal, the specific power of the power electronics is given as 14.3 kW/kg with an efficiency of 95% . The calculation of cable mass can be long process but in order to simply this a power density of 16 kg/m with an efficiency of 98% is assumed (Pornet 2017).

$$m_{EPS} = m_{gen} + m_{cable} + m_{pe} + m_{em} \tag{3.18}$$

$$\eta_{EPS} = \eta_{gen} \cdot \eta_{cable} \cdot \eta_{pe} \cdot \eta_{em} \sim 80\% \tag{3.19}$$

$()_{gen}$ electric generator
$()_{cable}$ distribution cable
$()_{pe}$ power electronics
$()_{em}$ electric motor

Using (3.18) and (3.19) on can calculate the total mass of the EPS if the required power is known. From (3.19) it is evident that electric propulsion system is more efficient compared to HPS. However, HPS is superior to EPS in power density as it is apparent from Table 3.2.

3.3 Gas Turbine Engine

A Gas Turbine (GT) engine is required for the Turbo-hydraulic/electric concept. They supply the principal power by driving the electric generator or the hydraulic pump. The shaft power of the GT engine is converted in to hydraulic or electric power. There are mainly three types of GT engines that can be used for this scenario and they are Turbofan, Turboshaft and Turboprop. Turbojet is excluded from the list because it consumes more fuel compared to the aforementioned engines and also more operational requirements.

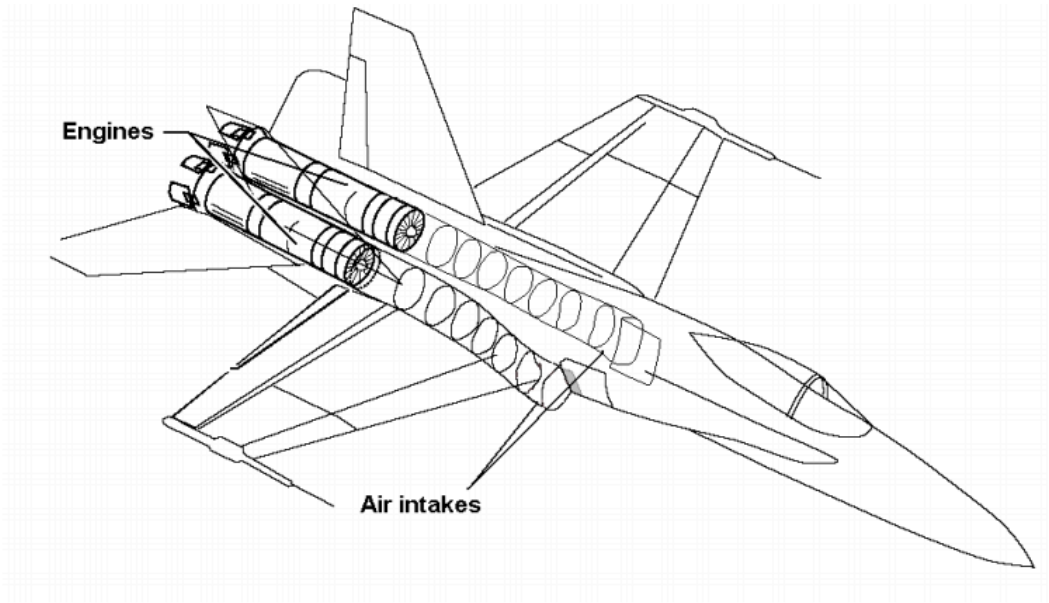

Figure 3.7 Submerged air intake of a fighter jet (Roy 2012)

In a fully Turbo-hydraulic/electric concept, the motors produce the entire thrust. Therefore, the GT engines are placed inside the aircraft. In this research an Airbus 320 aircraft is used as a reference aircraft. The engine intake needs to be placed in the fuselage in the shape of a scoop. This type of intake is defined as the submerged intake. This intake after further analysis can be positioned optimally in order to ingest boundary layer which reduces drag. This process is one the techniques used in Airbus Concept Plane according to Rostek (2015) to increase efficiency of the aircraft. They are frequently used in fighter jets.

3.3.1 Turboprop Engine

A turboprop engine is one of the choices for this configuration since, the intake area is inadequate for a turbofan engine. The turboprop engine consists of two main components, core engine and propeller. The propeller is connected to core engine using a drive shaft. This shaft will now be connected to the hydraulic pump or the electric generator. As explained in Chapter 3.1, the turboprop engine is placed in the centre of the aircraft.

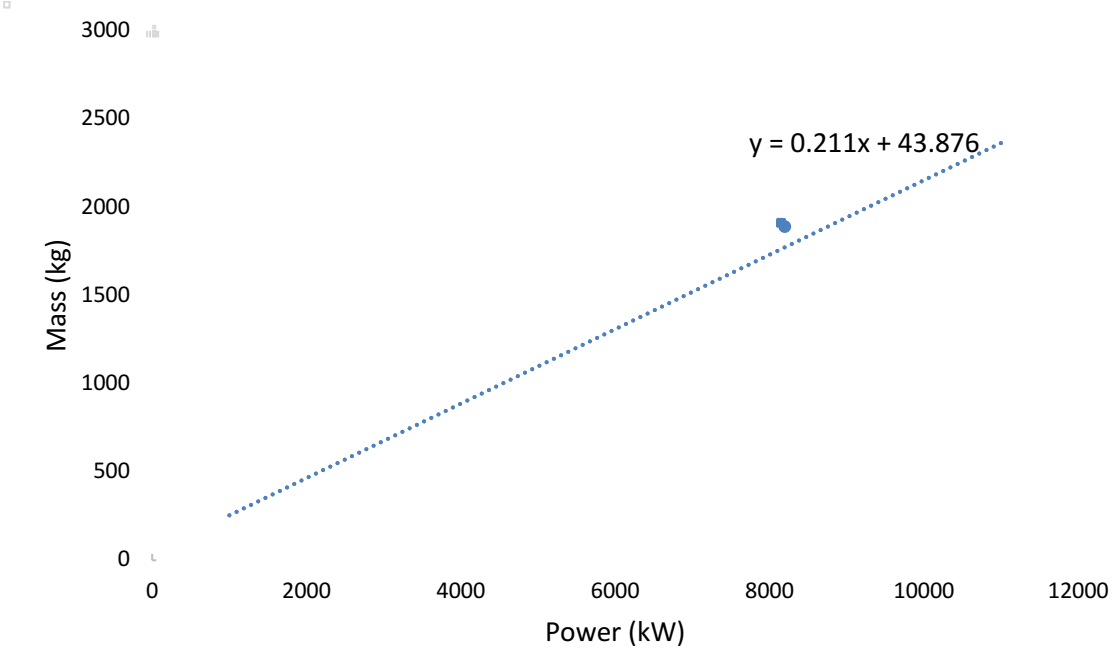

Figure 3.8 Turboprop engine mass statistic

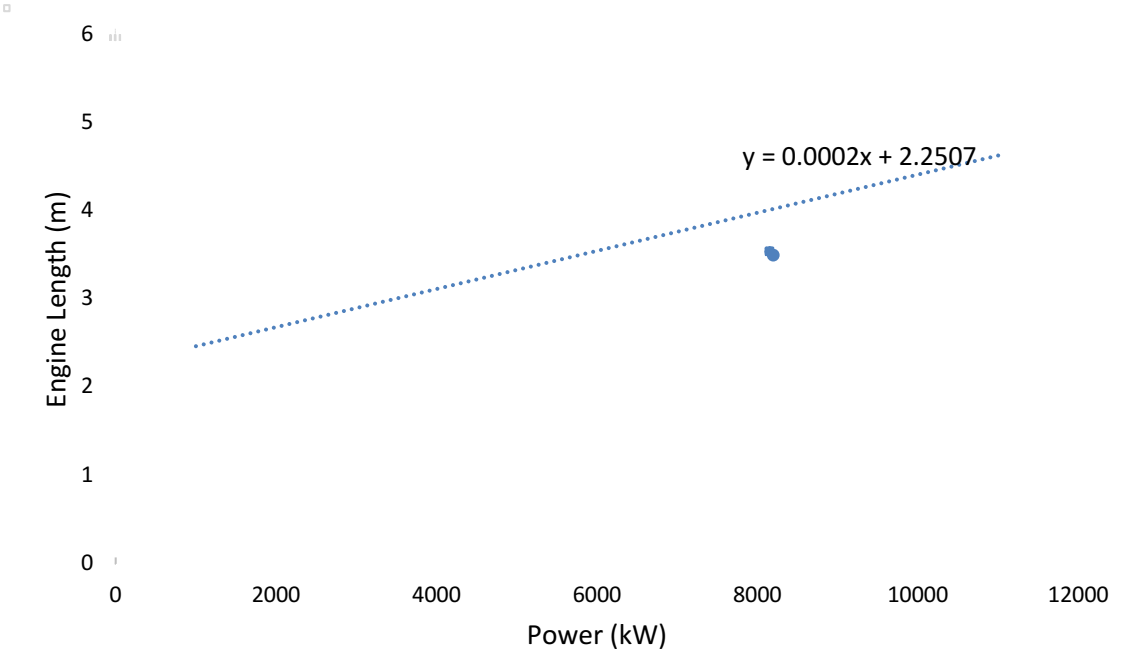

Figure 3.9 Turboprop engine length statistic

$$m_{TP} = 0.211 \cdot P_{s,TO} + 43.876 \tag{3.20}$$

$$l_{TP} = 0.0002 \cdot P_{s,TO} + 2.2507 \tag{3.21}$$

The data (Koppe 2012) from over 15 turboprop engines were used to plot Figure 3.8 and 3.9 with linear correlation. The R-squared value for Figure 3.8 is 65%. It commonly said that a minimum of 70% is a good value. For the purpose of this thesis, it is assumed that the value of R-squared is optimum. Once the power required is calculated, (3.20) and (3.21) can be used to calculate the turboprop engine mass (m_{TP}) and length (l_{TP}). The engine mass can later be utilized to calculate the operating empty mass of the aircraft. A crucial parameter of the turboprop engine that is required for aircraft design is the Power Specific Fuel Consumption ($PSFC$). The PSFC is unique to an engine and is provided by the engine manufacturer. According to Koppe (2012), it can be approximated for an engine using the Overall Pressure Ratio (OPR), Turbine Entry Temperature (T_{ET}) and the required static sea-level take-off power ($P_{s,TO}$). Since, each of these parameters are different for each engine, the Europrop TP 400 engine is used as a benchmark. Europrop TP 400 was selected because it produces thrust high thrust and it is one of the most recently developed aircraft.

Table 3.3 Europrop TP400 engine parameters

Parameter	**Value**
Power $P_{s,TO}$	8200 kW
Fuel flow rate $\dot{m}_f$	0.41625 kg/s
Turbine Entry Temperature T_{ET}	1550 K
Overall Pressure Ratio OPR	25

$$PSFC_{TP,Koppe} = 3.25369 \cdot 10^{-7} - \ln\left(P_{s,TO} \cdot OPR \cdot T_{ET}\right) \cdot 1.00060 \cdot 10^{-8} \quad (3.22)$$

$$PSFC_{TP,literature} = \frac{\dot{m}_f}{P_{s,TO}} \quad (3.23)$$

Table 3.4 PSFC calculation results for TP 400 engine

Method	Result
Koppe	6.03E-8 kg/W/s
Literature	5.07E-8 kg/W/s
Average	5.55E-8 kg/W/s

The parameters of the aforementioned engine were extracted from Teal (2017) and Schwarze (2014) and are given in Table 3.3. The PSFC for the Europrop TP400 engine can be calculated using (3.22) and (3.23). (3.23) is common literature method where fuel consumed by the engine($\dot{m}_f$) is divided by Power to calculate the PSFC. Since the results from both the methods differ, an average is calculated and will be used.

3.3.2 Turboshaft Engine

Another choice of gas turbine engine for this propulsion concept is the turboshaft engine. The main principle of the turboshaft engine is to provide more shaft power than jet thrust, similar to a turboprop engine. The important difference between the two engines are that unlike the turboprop engine, the turboshaft engine is not designed to support the loads created by a rotating propeller since the propeller is not attached to the engine. Typically, a turboshaft engine is attached to a transmission that embedded in the structure to support the loads. This can be beneficial to the turbo-electric/hydraulic propulsion system concept since the gas turbine engine is attached directly to a hydraulic pump or an electric generator.

$$m_{TS} = 2.5401 \cdot \left(P_{s,TO} \cdot 1.341022\right)^{0.585} \quad (3.24)$$

$$PSFC_{TS} = 2.2381 \cdot \left(P_{s,TO}\right)^{-0.21} \quad (3.25)$$

The mass estimation and performance of the turboshaft engine is carried out according to Stückl (2016). The mass of turboshaft engine (m_{TS}) is calculated using (3.24) where power is inputted in kW. The $PSFC_{TS}$ is calculated using (3.25) in lb/shp/hr and the power is inputted in shp. Both the parameters are determined based on a statistical correlation.

4 Aircraft Design Methodology

In this research, Aircraft Design plays a crucial role in analysis. Diverse propulsion system techniques were applied to account fuel burn, costs and environmental impact. Tools such as PreSTo for turboprop and turbofan equipped aircraft were utilized. These tools were created by AERO group at Hamburg University of Applied Sciences for research purposes. The aircraft design method used in this thesis follows the Aircraft Design lectures series by Scholz (2019**).** Three different propulsion system architectures were analysed with two distinct propulsion systems powered by three different gas turbine engines, summing up to ten different configurations.

4.1 Requirements

As mentioned earlier, the Airbus 320 aircraft is used as a reference aircraft. The Airbus 320 family of aircraft have several versions of the model to suit demands of the customers. The model A320-200 is chosen along with the CFM 56-5B4 engines configuration. This configuration was chosen mainly due to the availability of data. The principal idea of the thesis is to compare the aforementioned new propulsion concepts with an existing aircraft. Therefore, the Top-Level Aircraft Requirements (TLAR) of the A320 aircraft will be used to start the aircraft design procedure.

Table 4.1 Top level aircraft requirements of A320 (Airbus 2019)

Requirement	**Value**
Number of Passengers n_{PAX}	180
Range R	1700 NM
Cruise Mach Number M_{CR}	0.78

From Table 4.1 and Figure 4.1, the TLARs for this research are expressed. In the following aircraft design, it is assumed that all aircraft have a fuselage and other dimensions similar to that of A320. This is done because the thesis focuses mainly on effects of new propulsion system concepts on aircraft design. Therefore, using the parameters of the A320, a similar aircraft is redesigned without making any modifications. The redesigned aircraft is then installed with various introduced propulsion concepts. The aircraft parameters will then be compared with the A320 and the initial redesign of the A320 aircraft.

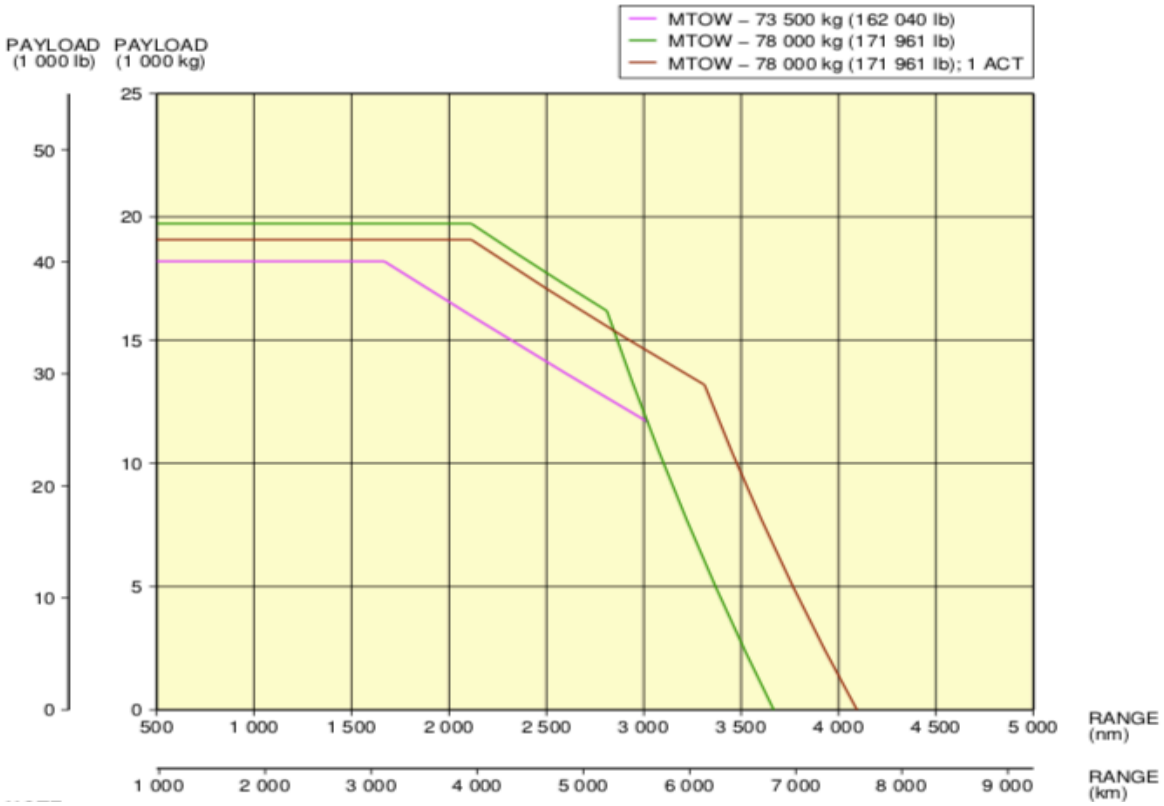

Figure 4.1 Payload versus Range diagram of A320-200 (Airbus 2019)

4.2 Turbo-Electric/Hydraulic Propulsion

As explained previously, the turboprop engines are buried inside the fuselage of the aircraft. Also, the propellers will be driven by the motors using hydraulic or electric power. Therefore, the preliminary sizing tool used for propeller aircraft is used here. This tool contains all the required equations for aircraft design of propeller aircraft and is available in Scholz 2008. The PreSTo tool for turboprop aircraft mainly contains of Preliminary Sizing modules that helps in calculating the simple parameters of an aircraft. Figure 4.2 shows the overall working of this tool. This tool has been modified to match the requirements of this thesis. Initially, three parameters should be selected. The type of propulsion is the first selection option. It includes turbo-hydraulic and turbo-electric option. Depending on the selection of propulsion system type, the mass estimation of the aircraft is carried out. Furthermore, the number of engines should be selected. This option was added to enable the study of distributed propulsion system. The $sin\gamma$ value changes with the number of engines. In the end, the type of gas turbine engine is chosen. The options are turboprop and turboshaft. The mass estimations change accordingly.

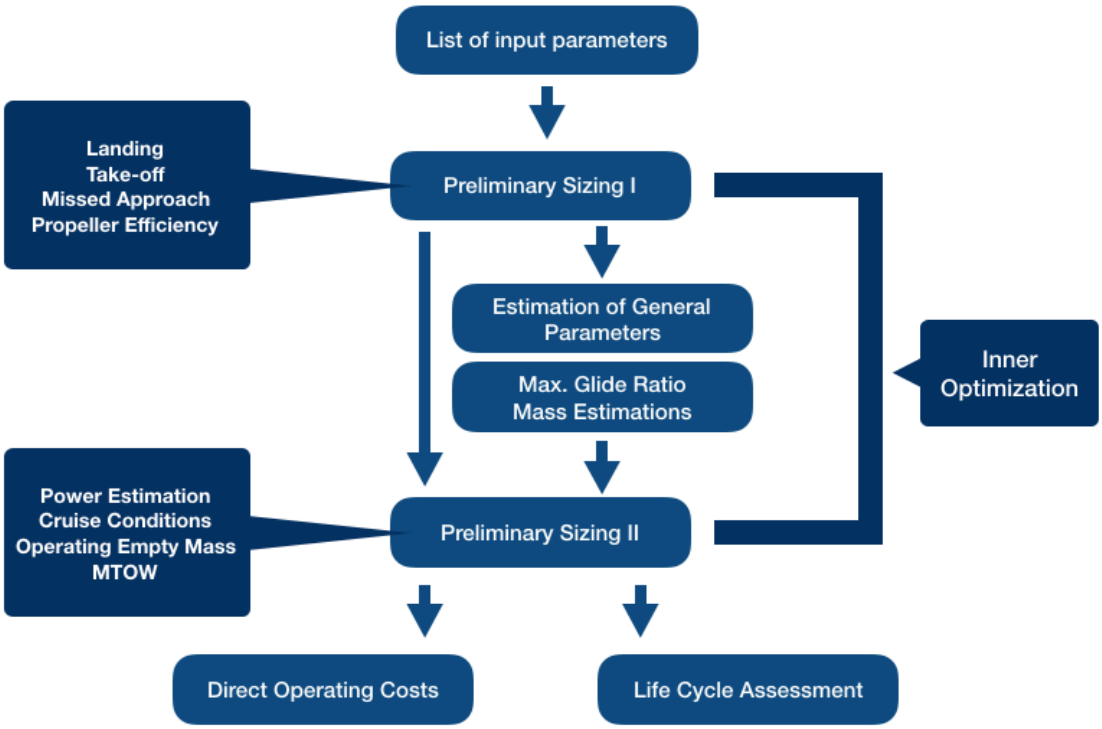

Figure 4.2 Aircraft Design method for Turbo-electric/hydraulic propulsion

In this chapter, the working of the tool and the important formulae used will be briefly described along with values. For detailed explanation of the calculations, one can refer to the lecture notes of Scholz (2019). All the A320-200 data are taken from Airbus (2019) and OPerA tool developed along with Nita (2013). Initially, redesign of the A320 is carried out. This aircraft will be set as the baseline for comparison. The turbo-electric/hydraulic propulsion system aircraft will be compared to A320 aircraft by adjusting the results of TE/TH aircraft with the difference between baseline aircraft and A320 aircraft.

4.2.1 Landing Distance

$$V_{APP} = k_{APP} \cdot \sqrt{S_{LFL}} \tag{4.1}$$

$$\frac{m_{ML}}{S_W} = k_L \cdot \sigma \cdot C_{L,max,L} \cdot S_{LFL} \tag{4.2}$$

$$\frac{m_{MTO}}{S_W} = \frac{\frac{m_{ML}}{S_W}}{\frac{m_{ML}}{m_{MTO}}} \tag{4.3}$$

Table 4.2 A320 data for landing distance (Nita 2013)

Parameter	Value
Landing field length S_{LFL}	$1480\ m$
Approach factor k_{APP}	$1.818\ \sqrt{m/s^2}$
Factor k_L	$0.122\ kg/m^3$
Relative Density σ	1
Max. lift coefficient landing $C_{L,max,L}$	3.14
Mass ratio, landing-take-off $\frac{m_{ML}}{m_{MTO}}$	0.88

The approach speed can be related to the landing field distance using statistics. The main value obtained from this section is the wing loading at maximum take-off mass ($\frac{m_{MTO}}{S_W}$). This can be achieved using (4.1), (4.2) and (4.3) and the values given in Table 4.2. All the values given in the Table 4.2, were calculated for A320.

4.2.2 Take-off Distance

$$\frac{P_{s,TO}}{m_{MTO}} = a \cdot \frac{m_{MTO}}{S_W} \tag{4.4}$$

$$a = \frac{k_{TO} \cdot 1.2 \cdot V_{s,1} \cdot g}{S_{TOFL} \cdot \sigma \cdot C_{L,max,TO} \cdot \eta_{P,TO} \cdot \sqrt{2}} \tag{4.5}$$

k_{TO} factor
$V_{s,1}$ stall speed, take-off configuration
$\eta_{P,TO}$ propeller efficiency during take-off
a slope

The input data for this block are the take-off field length (S_{TOFL}) and the maximum lift coefficient in take-off configuration ($C_{L,max,TO}$). By inputting these data, one can obtain the power to weight ratio as a function of wing loading. This can be calculated using (4.4), (4.5) and the result from (4.3).

Table 4.3 A320 data for take-off distance (Nita 2013)

Parameter	Value
Take-off field length S_{TOFL}	$1767.84\ m$
Factor k_{TO}	$2.25\ m^3/kg$
Max. lift coefficient for take-off $C_{L,max,TO}$	2.24

4.2.3 Second Segment and Missed Approach

$$E_{TO} = \frac{C_{L,TO}}{C_{D,P} + \frac{C_{L,TO}^2}{\pi \cdot A \cdot e}} \tag{4.6}$$

$$\frac{P_{s,TO}}{m_{MTO}} = \left(\frac{n_E}{n_E - 1}\right) \cdot \left(\frac{1}{E_{TO}} + sin\gamma\right) \cdot \left(\frac{V_2 \cdot g}{\eta_{P,CL}}\right) \tag{4.7}$$

The aviation authorities have specific certification regulation for the climb gradient after the landing gear is fully retracted. The portion of the climb between the retraction of landing gear and flaps is known as second segment. They differ with the number of engines the aircraft is equipped with. The glide ratio in take-off configuration (E_{TO}) is calculated using the profile drag ($C_{D,P}$) and induced drag. The induced drag depends on the lift coefficient ($C_{L,TO}$), Aspect ratio (A), and the Oswald efficiency factor (e). The power to weight ratio at take-off configuration is calculated using (4.7), where the number of engines (n_E) play a significant role. V_2 is the take-off safety speed.

Table 4.4 A320 data for second segment and missed approach (Nita 2013)

Parameter	Value
Aspect Ratio A	9.5 m
Number of engines n_E	2 and 4
Climb angle (second segment) $sin\gamma$	0.024
Climb angle (missed approach) $sin\gamma$	0.021

When an aircraft landing is aborted, the aircraft is required to climb immediately for a second approach. The drag is higher compared to second segment climb since the landing gear is fully extended. The equation for calculating the power to ratio for this configuration changes as seen in (4.8).

$$\frac{P_{s,TO}}{m_{MTO}} = \left(\frac{n_E}{n_E - 1}\right) \cdot \left(\frac{1}{E_L} + sin\gamma\right) \cdot \frac{m_{ML}}{m_{MTO}} \cdot \left(\frac{V_2 \cdot g}{\eta_{P,CL}}\right) \tag{4.8}$$

4.2.4 Cruise

Cruise segment of the flight is crucial in aircraft design since the majority of the flight time is cruise. It is assumed that the aircraft is on a straight flight at cruise altitude. Similar to the previous section, the wing loading and the power to weight ratio has to be found for the cruise flight.

$$E_{max} = k_E \cdot \sqrt{\frac{A}{S_{wet}/S_w}} \tag{4.9}$$

Initially, the maximum lift to drag ratio (E_{max}) if found using (4.9) and it depends on the k_E factor, aspect ratio and wetted area relative to wing area (S_{wet}/S_w). By inputting the data of A320, we obtain E_{max}.

$$\frac{C_L}{C_{L,md}} = \frac{1}{\left(\frac{V}{V_{md}}\right)^2} \tag{4.10}$$

$$E = \frac{2E_{max}}{\frac{1}{\left(\frac{C_L}{C_{L,md}}\right)} + \left(\frac{C_L}{C_{L,md}}\right)} \tag{4.11}$$

Using (4.10), one can determine the ratio between lift coefficient and minimum drag lift coefficient ($C_{L,md}$) using the ratio between velocity and velocity of minimum drag flight (V_{md}). According to Nita 2008, for propeller driven aircraft the value of V/V_{md} is approximately equal to 1. Therefore, by inputting the value of V/V_{md} in (4.11), it is understood that E is equal to E_{max} . By inputting the already calculated values needed in (4.11), the lift to drag ratio of the aircraft can be obtained.

The power variation of the gas turbine engine with height is important factor while calculating the parameters for cruise. According to Nita (2008), for turboprop engine this factor can be expressed using the ratio between power during cruise and power during take-off segments ($P_{CR}/P_{S,TO}$).

$$\frac{P_{CR}}{P_{S,TO}} = A \cdot M^m \cdot \sigma^n \tag{4.12}$$

In (4.12) A , m and n are the coefficients to find the power variation of the engine with height. These coefficients are derived from statistics from evaluation of generic engines. For detailed explanation about the derivation, Nita (2008) should be referred. The Mach number (M) is the cruise Mach number of A320. The power to weight ratio must be found using (4.13).

$$\frac{P_{s,TO}}{m_{s,TO}} = \frac{V_{CR} \cdot g}{P_{CR}/P_{s,TO} \cdot E \cdot \eta_{P,CR}} \tag{4.13}$$

Table 4.5 Data for cruise flight segment (Nita 2008 & Nita 2013)

Parameter	Value
Relative wetted area S_{wet}/S_w	6.299
k_E factor	14.31
Factor A	1.371
Factor m	0.101
Factor n	0.885
Mach number	0.78

$$V_{CR} = M \cdot a \tag{4.14}$$

$$\frac{m_{MTO}}{S_W} = \frac{C_L \cdot M_{CR}^2 \cdot \gamma \cdot p(h)}{2 \cdot g} \tag{4.15}$$

γ heat capacity ratio
$p(h)$ pressure at cruise altitude

The cruise speed (V_{CR}) of the aircraft is calculated using (4.14) as a product of Mach number (M) and speed of sound (a). M is derived from the cruise Mach number of A320. a is calculated using the cruise temperature and altitude. The wing loading is calculated for cruise flight using (4.15). Using the wing loading and power to weight ratio calculated until now for various segments of flight, a matching chart can be constructed. The chart is useful to determine the design point of an aircraft.

4.2.5 Propeller Sizing and Efficiency

$$L = \frac{P}{\sigma \cdot \rho_0 \cdot S_D} \tag{4.16}$$

$$\eta_P = (-0.0002L + 0.9001) \cdot \left(1 - e^{-\left(0.134\, L^{-0.3008}\right)V}\right) \tag{4.17}$$

Since the electric/hydraulic motors are equipped with propellers, the efficiency of the propellers is of paramount importance during all segments of flight. The propeller efficiency (η_P), is expressed in (4.17) as a function of disc loading (L) and airspeed (V). The propeller area (S_D), is calculated using the diameter of the propeller. The efficiency of the propeller decreases with the decrease in propeller diameter, although it decreases the load on the structure.

An important parameter to be considered while designing a propeller is the blade tip speed. High Mach number on the blades can lead to reduction in efficiency. Most of the turboprop aircraft fly in a relatively lower altitude dude to this reason. To solve this complication, the propeller blades can be swept which in turn reduces the Mach number and noise. In order to have a statistical approach for propeller sizing, the propeller diameter of the Smart Turboprop aircraft designed by Scholz (2014) is 7 m and the propeller diameter of Airbus 400M aircraft is 5.35 m (Teal 2017). These two aircraft were chosen because of their similarity to the requirements of A320.

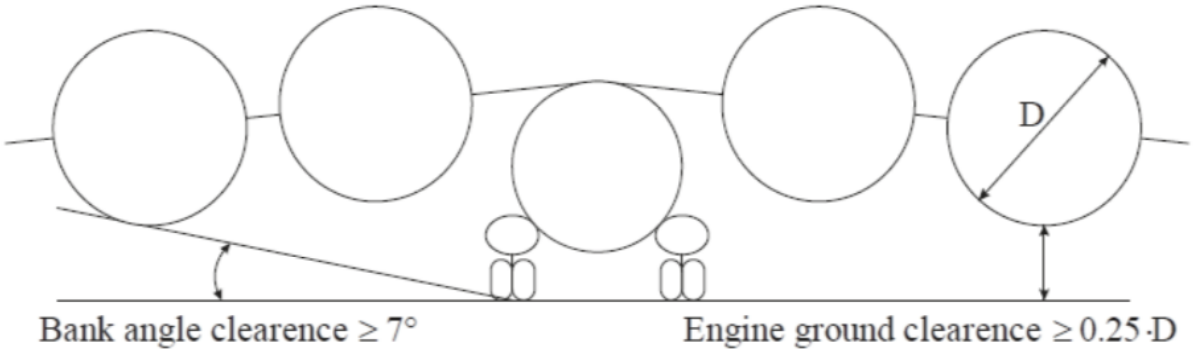

Figure 4.3 Propeller sizing requirements (Scholz 2014)

The other requirements according to Scholz (2014) for a propeller driven aircraft are ground clearance with the propeller should be a minimum of 25% of the propeller diameter and the minimum bank clearance angle must 7°. From the A320 data in Airbus (2019), the wing ground clearance is 3.78 m. Assuming the propeller hub is placed in the wing line and by taking into consideration of the requirements, the maximum propeller diameter can be calculated to be 5.67 m. As mentioned previously, the higher propeller diameter increases efficiency. Therefore, the propeller diameter is taken to be 7 m. The propeller-ground clearance complication can be solved by increasing the height of the landing gear. This leads to an increase in overall mass of the aircraft, but it is ignored in this study.

4.2.6 Mass Estimation

The mass estimation of the entire aircraft is a crucial section in aircraft design. The ultimate aim is determining the maximum take-off mass ($MTOW$) of the aircraft.

$$B_S = \frac{\eta_P \cdot E}{PSFC \cdot g} \tag{4.18}$$

The Breguet range factor (B_S) is found initially using (4.18). The parameters required are calculated in the previous chapters. The Breguet factor for flight time (B_t) is also found by dividing B_S by the cruise speed (v_{CR}).

$$M_{ff,CR} = e^{-\frac{R}{B_S}} \tag{4.19}$$

The mission fuel fraction for cruise ($M_{ff,CR}$) should to be calculated with (4.19). The value of range (R) is taken from Table 4.1. Similarly, the mission fuel fraction for reserve ($M_{ff,RES}$) is calculated by replacing R with R_{RES} in Equation 4.19. The value for R_{RES} for a domestic flight is 200 nautical miles. The mission fuel fraction for loiter ($M_{ff,LOI}$) is calculated by replacing R with loiter time (t_{loiter}) with a value of 2700 s (domestic flight) and B_S with B_t in Equation 4.19.

Table 4.6 Mass fractions of different light phases

Phase	Index	Value
Taxi $M_{ff,taxi}$	T	0.995
Take-off $M_{ff,TO}$	TO	0.995
Climb $M_{ff,CLB}$	CLB	0.985
Descent $M_{ff,DES}$	DES	0.985
Landing $M_{ff,L}$	L	0.995

$$M_{ff,STD} = M_{ff,TO} \cdot M_{ff,CLB} \cdot M_{ff,DES} \cdot M_{ff,L} \cdot M_{ff,CR} \tag{4.20}$$

$$M_{ff,res} = M_{ff,CLB} \cdot M_{ff,RES} \cdot M_{ff,DES} \cdot M_{ff,LOI} \tag{4.21}$$

$$M_{ff} = M_{ff,res} \cdot M_{ff,STD} \tag{4.22}$$

The mission fuel fraction (M_{ff}) is a parameter that is used to calculate the fuel consumed for a complete flight. In order to calculate M_{ff}, the mission fuel fraction of all the flight phases must be taken in to account. This is shown in Table 4.6 and previously. The standard mission fuel fraction ($M_{ff,STD}$) and the reserve mission fuel fraction ($M_{ff,res}$) are multiplied to calculate M_{ff}.

$$m_{PL} = m_{PAX} \cdot n_{PAX} + m_{cargo} \tag{4.23}$$

The mass of payload (m_{PL}) is the sum of product of number of passengers (n_{PAX}) and mass of on passenger (m_{PAX}) and mass of cargo (m_{cargo}). This aircraft is designed for 180 passengers and mass of a passenger along with their bag is 93 kg. It is assumed that this aircraft is designed only for passenger transport, therefore mass of cargo is ignored. Although, the A320 aircraft is designed to carry cargo, the MTOW for the redesigned aircraft is taken from Figure 4.1 for the exact payload mass of this aircraft. Therefore, the total payload mass is equal to 16740 kg.

$$m_{OE} = m_{fus} + m_W + m_H + m_V + m_{LG} + m_{SYS} + m_{propulsion} + m_{cor} \tag{4.24}$$

$$m_{propulsion} = m_{GT} + m_{EPS} \tag{4.25a}$$

Or,

$$m_{propulsion} = m_{GT} + m_{HPS} \tag{4.25b}$$

$$m_{cor} = m_{OE,A320} - \left(m_{fus} + m_W + m_H + m_V + m_{LG} + m_{SYS} + m_{propulsion}\right)_{A320} \tag{4.26}$$

Table 4.7 Component mass of A320 (Nita 2013)

Component	**Mass**
Fuselage m_{fus}	$9235.12\ kg$
Wing m_W	$6189.53\ kg$
Horizontal Tail m_H	$635.83\ kg$
Vertical Tail m_V	$463.00\ kg$
Landing Gear m_{LG}	$2247.42\ kg$
Systems m_{SYS}	$7685.94\ kg$
CFM 56-5B4 with Nacelle $m_{propulsion}$	$3886.34\ kg$
Correction m_{cor}	$7014.46\ kg$

Typically, the operating empty mass is calculated using the ratio between m_{OE} and m_{MTO}. Since this aircraft is redesigned only for integrating a new propulsion system, it is assumed that all the other components of the A320 is the same for the redesigned aircraft. The operating empty mass (m_{OE}) of the aircraft is calculated using (4.24). All the values used in this equation is taken from the A320 aircraft, since it is assumed that redesigned aircraft have similar component masses. The propulsion system mass ($m_{propulsion}$) can have three values. Initially, for the first redesigned aircraft the mass of the turbofan engine given in Table 4.7 is used. For the Turbo-hydraulic/electric propulsion system aircraft, Equation (4.25a, b) can be used. The mass of the gas turbine engine (m_{GT}) can either be mass of turboprop engine (chapter 3.3.1) or mass of turboshaft engine (chapter 3.3.2) depending on the configuration of the aircraft. The operating empty mass of the A320 aircraft is 41244 kg. The mass of most of the components that constitute to m_{OE} of A320 have been found. In order for the redesigned aircraft to have the same components mass, the correction mass (m_{cor}) is introduced and added to the m_{OE} of the redesigned aircraft.

$$m_{MTO} = \frac{m_{PL} + m_{OE}}{M_{ff}} \tag{4.27}$$

$$\frac{P_{s,TO}}{n_E} = \frac{m_{MTO}}{n_E} \cdot \frac{P_{s,TO}}{m_{MTO}} \tag{4.28}$$

Typically, the m_{MTO} is calculated using the relative operating empty mass. The relative operating empty mass is the ratio between m_{MTO} and m_{OE}. This ratio can be determined using statistical data and from various literature. However, when this method was implemented, a "circular reference" error was identified in excel. Therefore, another solution was found to calculate the m_{MTO}. The m_{MTO} can be calculated using (4.27). The power required for take-off by one engine ($P_{s,TO}/n_E$), is calculated by multiplying the power to weight ratio with maximum take-off mass divided by the number of engines. This value of power to weight ratio is used as an input to determine the mass of HPS and EPS and the complete mass estimation is iterated.

4.2.7 Comparison of Parameters

Table 4.8 Comparison of aircraft parameters

Parameter	A320 aircraft value	Redesigned aircraft value	Deviation
Wing surface area (m^2)	122.4	112.4	-8%
Maximum take-off mass (kg)	73500	72544	-9.5%
Operating empty mass (kg)	41244	41244	0%
Wing loading (kg/m^2)	600.49	645.2	$+7.4\%$
Cruise Altitude (ft)	38000	29425	-22%

In Table 4.8, the values of all the important parameters of A320 aircraft is compared with the redesigned baseline aircraft. In most cases the deviation is less than 10 %, this shows that the aircraft design method is effective. The significant difference in cruise altitude can be caused due to the propeller driven aircraft PreSTo tool. The tool utilizes the relative power ratio which mainly depends on the statistical data of propeller driven engines. Since the cruise of propeller driven engines are lower than turbofan engines, the significant deviation can be justified. By determining the parameters of a baseline aircraft, it is easier to compare the results.

4.3 Partial Turbo-Electric/Hydraulic Propulsion

The Partial Turbo-electric/hydraulic propulsion concept is a combination of gas turbine and electric/hydraulic motors with propellers. In this research, in order to modify the configuration of the aircraft to partial turbo-electric/hydraulic propulsion, two additional motors with propellers are added. The motors are placed between the mid-wing section and wingtip. The motors are powered by the shaft off-take power extracted from the low-pressure turbine of the turbofan engine. The power extracted is transferred to the motor using similar method used in the completely turbo-electric/hydraulic propulsion concept. The crucial advantage for this concept is the increased fuel efficiency due to increase in effective engine by-pass ratio. This is an obvious advantage since, size of the engine core remains the same while the fan area increases drastically.

The shaft power is extracted from the low-pressure turbine using the Accessory Gearbox. In commercial aircraft engines, this mechanical device is used to drive the hydraulic pumps, electric generators and compressors for air-conditioning. The fuel consumption required due to shaft power off-takes can be calculated by two methods analysed in Scholz (2014). This is presented in chapter 3.2.

It is assumed that, the engine produces the required thrust for an aircraft to fly and produces additional shaft power to influence the supplementary systems. The objective is to utilize this additional power produced to fuel another electric/hydraulic motor which produces thrust. The amount of power extracted from the engine is limited due to the capability and efficiency of the engine. The ratio of take-off thrust, and cruise thrust can be defined as a thrust setting. By changing the thrust setting during cruise, also while powering the additional motors, one can identify the savings in fuel and notice the change in overall efficiency.

The additional motors and their components increase the overall mass of the aircraft. The increase in mass may nullify the positive effects of this concept. Therefore, in order to preserve the positive effects of this concept, the mass of motor and components are kept to a minimum. During a flight cycle, cruise segment will only require significantly less thrust for over a long period of time. Accordingly, in this research, the additional motors are utilized only during the cruise segment.

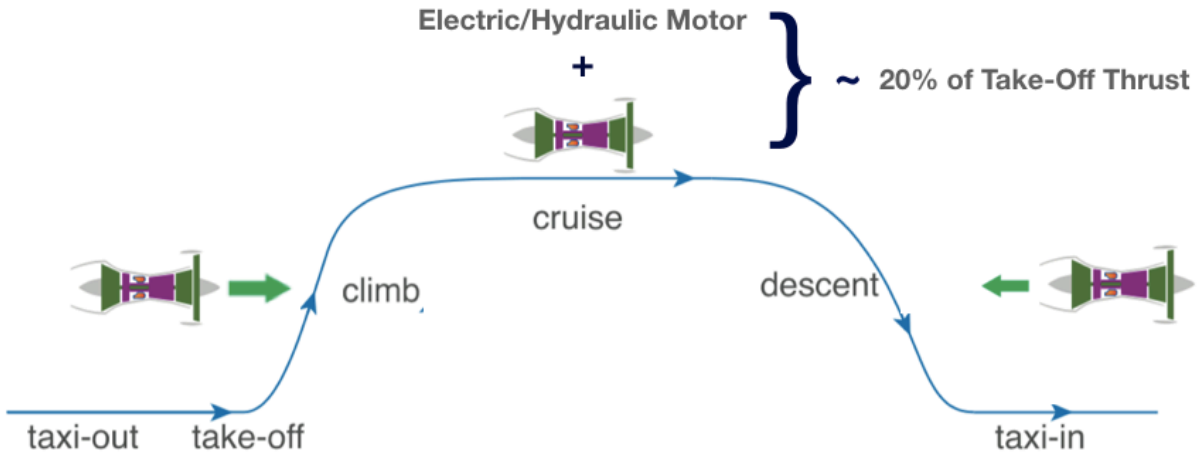

Figure 4.4 Operation cycle of partial TH/TE (adapted from Ang 2018)

In the analysis of the Turbo-electric/hydraulic propulsion concept, the Pre-STO tool for propeller aircraft was edited to match the requirements of the aforementioned concept. However, for the analysis of partial Turbo-electric/hydraulic propulsion concept, the Pre-STO tool for turbofan engine equipped aircraft was utilized. In the Pre-STO tool, three additional modules were added to present the calculations of mass estimations of the propulsion concepts, aircraft and the estimation of the new SFC.

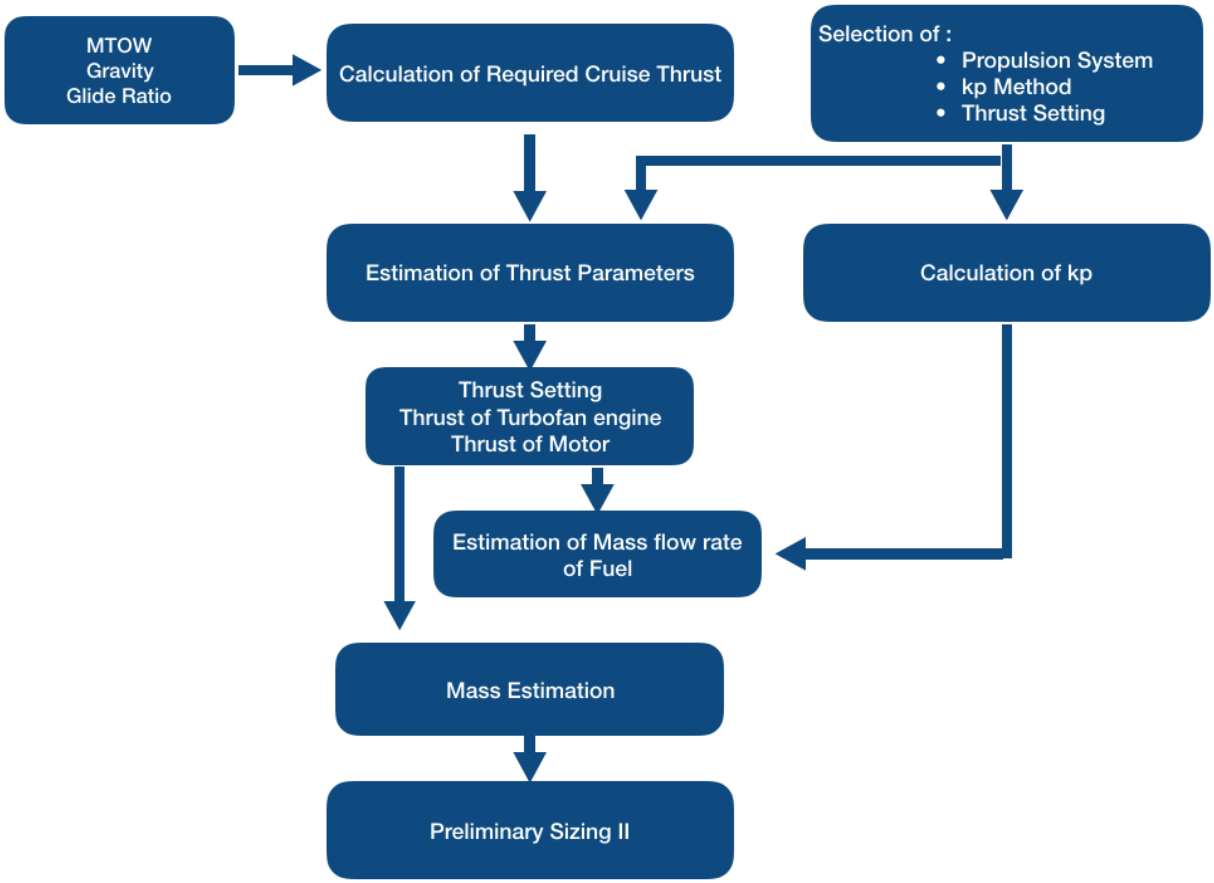

Figure 4.5 Partial Turbo-electric/hydraulic propulsion concept calculation method

The main difference between Pre-STO tool for propeller driven and turbofan engine aircraft is that one is measured in power and the other in thrust. Initially, the type of propulsion system architecture is chosen. The options are between turbo-electric and turbo-hydraulic systems. Furthermore, the level of thrust should be chosen from a drop-down box. In this drop-down box, the values 10%, 15%, 16% and 18% are provided. These values represent the amount of thrust produced by the turbofan engine to the take-off thrust. Finally, the kp method should be chosen between Turbomatch and Scholz method.

When the selections have been made, a set of initial parameters are automatically calculated. These parameters include the percentage of thrust produced by motor and turbofan engine, the fuel mass flow rate and the new TSFC. These values will then be iterated to determine a more accurate value. The mass estimation of the motor and the complete propulsion system depends on the value of thrust produced by the motor calculated in the previous step. The complete mass estimation is then introduced in the Preliminary sizing II module and the complete calculation model is automatically iterated. The new TSFC calculated will be inputted for the DOC calculation that provides. The new TSFC is not inputted in the preliminary sizing II module since the turbofan engine is designed with a specific TSFC and it cannot be changed. The trip fuel mass calculated in the DOC module is then used in the LCA calculation. The theory of the calculations involved in this tool is explained below.

Initially, the cruise thrust (T_{CR}) is calculated in order to determine the cruise thrust setting. This is done by assuming that the aircraft is in cruise condition where thrust equals drag and lift equals weight of the aircraft. Therefore, dividing weight of the aircraft by lift to drag ratio, required cruise thrust is obtained as shown in (3.29).

$$T_{CR} = D_{CR} \tag{4.29}$$

$$T_{CR} = \frac{W}{\frac{L}{D}} \tag{4.30}$$

$$T_{CR} = \frac{m_{aircraft} \cdot g}{\frac{L}{D}} \tag{4.31}$$

$$Thrust\ setting_{CR} = \frac{T_{CR}}{T_{TO}} \sim 0.2\ or\ 20\% \tag{4.32}$$

$m_{aircraft}$ is the mass of the aircraft and g represents the acceleration due to gravity. The product of both of them are used to determine the value of weight. According to Scholz (2014)**,** thrust setting for cruise is approximately 20% of the thrust setting for take-off. The result from the current aircraft further confirmed the aforementioned number. Since a baseline thrust setting has been established, it can be varied to identify the positive and negative impacts on the system. 18%, 16%, 15%, and 10% are analysed in this research. The thrust setting influences the amount of thrust produced by turbofan (T_{TF}) engine and motor (T_M). The two thrust parameters can be calculated using (4.33) and (4.34) for an example thrust setting of 15%.

$$T_{TF} = T_{CR} \cdot \frac{15\%}{20\%} \tag{4.33}$$

$$T_M = T_{CR} - T_{TF} \tag{4.34}$$

$$T_{Total} = T_{TF} + T_M \tag{4.35}$$

The thrust produced by the two propulsors are added to get the Total thrust (T_{Total}). This process is carried out to re confirm that $T_{Total} = T_{CR}$ .The mass flow rate of fuel consumed by turbofan engine ($\dot{m}_{F,TF}$) can be calculated using T_{TF} and Thrust specific fuel consumption of the engine ($TSFC_{CR}$) with (4.36)

$$\dot{m}_{F,TF} = T_{TF} \cdot TSFC_{CR} \tag{4.36}$$

$$\dot{m}_{F,M} = k_p \cdot P_{shaft\ off-take} \cdot TSFC_{CR} \tag{4.37}$$

The mass flow rate of fuel consumed by motor ($\dot{m}_{F,M}$) can be calculated using two methods according to Scholz (2014). In this research, both the methods are analysed. The first method is dependent on shaft power factor (k_p), power extracted from the shaft ($P_{shaft\ off-take}$) and $TSFC_{CR}$. In this method, k_p is calculated initially. It is based on a simulation of a turbofan engine using TURBOMATCH scheme. TURBOMATCH is a tool created by Cranfield University to simulate and model and engine and extract data points to unify a method to determine k_p. In the method defined by TURBOMATCH, k_p is mainly dependent on altitude and Mach number. The following equations are

$$k_p = a(h)M^2 + b(h)M + c(h) \tag{4.38}$$

with

$$a(h) = -3.5 \cdot 10^{-7} \frac{1}{m} h + 6.75 \cdot 10^{-3} \tag{4.39}$$

$$b(h) = 4.7 \cdot 10^{-7} \frac{1}{m} h - 1.208 \cdot 10^{-2} \tag{4.40}$$

$$c(h) = 1.0 \cdot 10^{-8} \frac{1}{m} h + 5.85 \cdot 10^{-3} \tag{4.41}$$

By inputting the values for Mach number (M) as 0.78 and altitude (h) equal to11524 m, k_p has a value of 0.0024203 N/W.

The shaft off-take power ($P_{shaft\ off-take}$) is dependent on required thrust of the motor (T_M) and the cruise speed of the aircraft (V_{CR}). The efficiency ($\eta_{hydraulic/electric}$) of transmission of power from the shaft to the electric motor should also be taken into account. $\eta_{hydraulic/electric}$, is explained in the third chapter. The Equation (4.42) is divided by 1000 in order to express the results in kilowatts.

$$P_{shaft\ off-take} = \frac{T_M \cdot V_{CR}}{\eta_{hydraulic/electric} \cdot 1000} \tag{4.42}$$

Using shaft off-take power, the mass estimations for hydraulic and electric propulsion systems are carried out. The mass estimations are then added to the MTOW of the aircraft that changes the (4.31) again and the results are iterated to obtain a correct value. The third expression in Equation (4.37), is the TSFC during cruise condition of the engine.

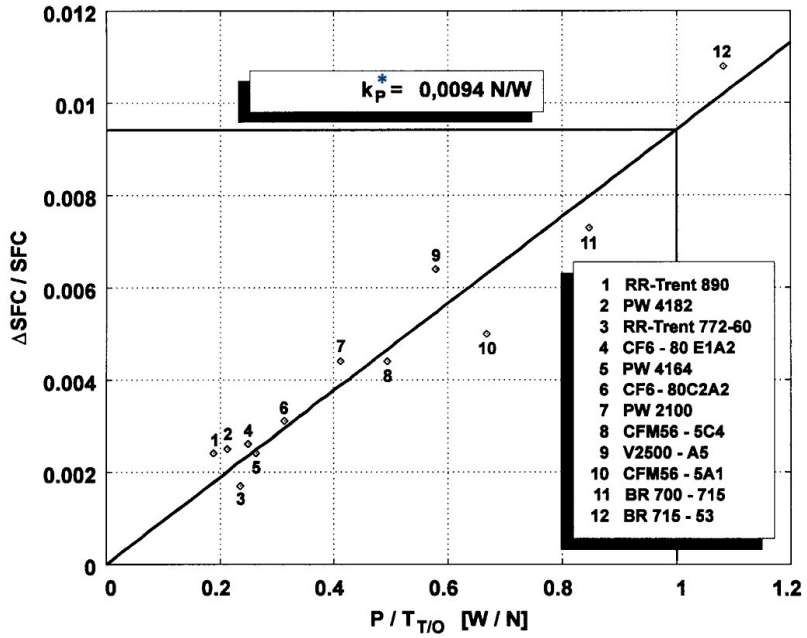

Figure 4.6 kp* obtained from plotting relative change in SFC (Scholz 2014)

The second method of determining the mass flow rate of fuel consumed by the motor is introduced by Scholz (2014). The previous method is a conventional approach compared to second method. In the second approach, Scholz defines a new shaft power factor k_p^* compared to the previous method. This factor is obtained by plotting each data point for various engines in different altitudes and Mach numbers. From the above graph, the value of k_p^* is equal to 0.0094 N/W. The new method of calculating $\dot{m}_{F,M}$ is given in (4.43) where the Power is divided by a unified thrust, which is the take-off thrust.

$$\dot{m}_{F,M} = k_p^* \cdot \frac{T_{CR}}{T_{TO}} SFC \cdot P_{shaft\ off-take} \tag{4.43}$$

$$k_p = k_p^* \cdot \frac{T_{CR}}{T_{TO}} \tag{4.44}$$

In (4.44) we can calculate the k_p using the second method. In this case, by inputting the values for cruise thrust and take-off thrust, a constant value is 0.0016 N/W is found for k_p. The value is constant since cruise thrust to take-off thrust ratio is approximately equal to 0.2.

$$\dot{m}_F = \dot{m}_{F,M} + \dot{m}_{F,TF} \tag{4.45}$$

$\dot{m}_F$, the total mass flow rate of fuel consumed by the whole propulsion system is the sum of the calculated fuel mass flow rates of motor and turbofan engine.

$$TSFC_{CR,new} = \frac{\dot{m}_F}{T_{Total}} \tag{4.46}$$

The new Thrust specific fuel consumption is calculated by dividing the new fuel mass flow rate by the total thrust found in (4.35). $TSFC_{CR,new}$ is then inserted in the DOC calculation to find the positive effects of this propulsion concept over the previous concepts.

$$T_M\ (\%) = \frac{T_{CR} - T_{TF}}{T_{TF}} \tag{4.47}$$

$$T_{TF,extra}\ (\%) = \left(1 + \frac{T_M\ (\%)}{\eta_{hydraulic/electric}}\right) \tag{4.48}$$

As mentioned previously, the turbofan engine has a limitation in terms of power extraction with shaft power off-take. It is assumed that the turbofan engine produces extra power to supply shaft off-take power. In order to calculate the extra power required by the engine to produce the required shaft power, certain parameters are required that can only be provided by the manufacturer. This might lead to a complicated task. Since the Equation (4.47) and (4.48) are ratios and both (engine and motor) would have the same local airspeed, one can assume that (4.48) is accurate.

Table 4.9 Comparison of aircraft parameters of redesigned aircraft with A320

Parameter	A320 aircraft value	Redesigned aircraft value	Deviation
Wing surface area (m^2)	122.4	110	-10%
Maximum take-off mass (kg)	73500	71334	-2.9%
Operating empty mass (kg)	41244	41244	0%
Wing loading (kg/m^2)	600.49	647	$+7.7\%$
Cruise Altitude (ft)	39000	37808	-3%

Table 4.9 contains the parameters of the A320 aircraft along with the deviation. Similar to the propeller driven aircraft, the results show less than 10% of deviation. Also, the cruise altitude is very close to the actual value of A320. This proves that the PreSTo tool for propeller driven aircraft was the cause of major deviation in cruise altitude in chapter 4.2.7.

4.4 Direct Operating Costs

The cost analysis of every aircraft designed in the previous chapters will be computed in this chapter. There are many different cost analysis models that can be used to estimate the costs of an aircraft operator and the model used in this thesis is Direct Operating Costs (DOC)Since cost is one of the biggest design drivers for engineers developing an aircraft and selling point to customers, it is important to evaluate the direct operating costs with optimum detail and accuracy with a simple method. The DOC method followed in this chapter is according to AEA 1989 a method (Scholz 2019).

$$C_{DOC} = C_{DEP} + C_{INT} + C_{INS} + C_F + C_M + C_C + C_{FEE} \tag{4.49}$$

(4.49) is method that DOC is calculated with. Various cost elements and aircraft parameters are utilized. The cost elements are defined briefly below. For detailed explanation, Scholz (2019**)** should be referred.

4.4.1 Depreciation Costs

$$C_{DEP} = \frac{P_{total}\left(1 - \frac{P_{residual}}{P_{total}}\right)}{n_{DEP}} \tag{4.50}$$

The depreciation costs (C_{DEP})of an aircraft is considered because the value of the aircraft decreases over the years in its service lifetime (n_{DEP}) of 14 years. The total price (P_{total}) is the acquisition price of an aircraft when it is new. P_{total} is the sum of delivery price, spares, engine and airframe prices. The delivery price can be calculated by various methods but in this case, the relevance of operating empty mass is significant. This is because additional mass is added due to propulsion system can be represented with m_{OE}. $P_{residual}/P_{total}$, is ratio obtained with statistical data and the value is 0.10.

4.4.2 Interest and Insurance Costs

$$C_{INT} = k_{INS} \cdot P_{total} \tag{4.51}$$

$$C_{INS} = k_{INS} \cdot P_{delivery} \tag{4.52}$$

Airlines often procure an aircraft with outside sources. Therefore, the interest costs (C_{INT}) are considered and total price of the aircraft is used to determine the value. For insurance costs (C_{INS}), the delivery price of the aircraft is used.

4.4.3 Fuel Costs

$$C_F = n_{t,a} \cdot P_F \cdot m_F \tag{4.53}$$

$$m_F = m_{MTO}(1 - M_{ff}) \tag{4.54}$$

In order to calculate the fuel costs (C_F), the mass of fuel must be calculated using (4.54). The number flight per year ($n_{t,a}$) must be calculated using an empirical formula derived in the AEA method by taking flight time (t_f) for one trip into account. By dividing the trip distance by the cruise velocity, one can approximate the flight time for one trip. The fuel price (P_F) is taken from IATA (2019). At the time of research, the fuel price was 0.37 /kg. The mass of fuel (m_F) is determined using (4.54) and by using the method in chapter 3.2.

4.4.4 Maintenance Costs

$$C_M = \left((t_{M,AF,f} + t_{M,E,f}) \cdot L_M + C_{M,M,AF,f} + C_{M,M,E,f}\right) \cdot t_f \cdot n_{t,a} \tag{4.55}$$

$t_{M,AF,f}$	maintenance man hours for airframe per flight hour
$t_{M,E,f}$	maintenance man hours for engine per flight hour
L_M	labor rate
$C_{M,M,AF,f}$	cost of material for airframe per flight hour
$C_{M,M,E,f}$	cost of material for engine per flight hour

An aircraft operator must always maintain it for making it airworthy. Large maintenance costs arise from spare parts and maintenance personnel working hours. Using the comprehensive approach (4.55), one can define the overall maintenance costs (C_M). While $C_{M,M,AF,f}$, defined mainly by the operating empty mass of the aircraft, $C_{M,M,E,f}$ is accounted by obtaining the number of shafts, compressors and other engine parameters. Therefore, by multiplying all these factors by the flight time (in hours) and number of flights per year, C_M is found. A few engine parameters are required for engine maintenance costs and they differ between turbo-fan, turboshaft and turboprop.

Table 4.10 Engine parameters of turbofan, turboprop and turboshaft

Parameter	Turbofan	Turboshaft	Turboprop
Overall Pressure Ratio	26.5	16	25
Number of Compressor stages	12	14	12
Number of Shafts	2	2	3

4.4.5 Staff Costs

$$C_c = (n_{CO}L_{CO} + n_{CA}L_{CA}) \cdot t_b \cdot n_{t,a} \tag{4.56}$$

The staff costs (C_c) for a commercial flight is calculated here. The number of cockpit crew (n_{CO}), for a short to medium haul flight would 2. The number of cabin attendants (n_{CA}), depends on the number of passengers as one cabin attendant is required per 50 passengers. In this case with 150 passengers recommended by Airbus, n_{CA} would be equal to 3. The above two factors are multiplied by their appropriate labor rates, block time (t_b) and number of flights per year. Block time is defined as the time since the chalks are removed in the origin airport and when they are placed back after landing in the destination airport.

4.4.6 Fees and Charges

$$C_{FEE} = C_{FEE,LD} + C_{FEE,NAV} + C_{FEE,GND} \tag{4.57}$$

A flight also incurs costs from fees and charges (C_{FEE}) from the airport. It is the sum of landing fees ($C_{FEE,LD}$), navigation fees($C_{FEE,NAV}$) and ground handling fees($C_{FEE,GND}$). They can be calculated using the AEA method.

After completing the calculations individually, all the costs are added together to find the direct operating costs of an aircraft annually. In this case, an example flight between Hamburg and Lisbon was used with a trip distance of 1190 NM. A 3D model is created to understand the division of costs of an aircraft.

4.5 Life Cycle Assessment

The design crucial design driver for an aircraft is its fuel efficiency, costs and aviation regulations that govern the overall design requirements. It is important to take into account of the environmental impact (EI) caused by the aircraft from the time of conceptualization till the end of life. The methodology followed here is created by Johanning (2013). A tool was created study the impact throughout all the phases of an aircraft by Johanning (2016). This tool was used to evaluate all the aircraft concepts proposed in this thesis. The working principle of the tool is briefly explained here.

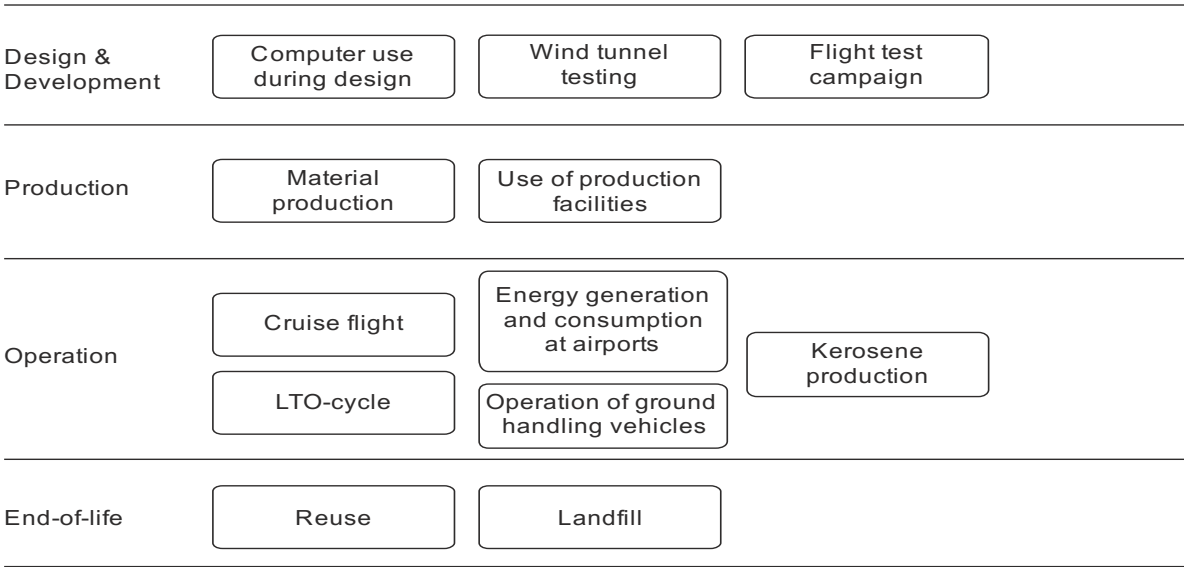

Figure 4.7 Processes considered in life cycle assessment (Johanning 2013)

All the input and output emissions that lead to climate change is normalized to CO_2-equivalent emissions. PKM is used as a functional unit. It stands for per passenger over one kilometre. The comparison is done using CO_2-equivalent per PKM. The tool uses the ReCiPe method which calculates 18 mid-point categories and 3 end-point categories. In this tool, the above processes are mainly considered for calculating the EI in terms of Single Score (SS). The SS is a summary of EI of an aircraft in one score which will be used for comparison. For the purpose of this thesis, CO_2 emissions during cruise flight, absolute share of CO_2 and single score will be determined.

Initially, a basic set of parameters are calculated. Then, all the inputs and outputs are calculated in terms of PKM from all the processes that are being considered. This leads to determination of results from the inventory analysis, that is magnitude of emissions. The mid-point and end-point categories are calculated next that provides single score along with the summary of impact assessment. The inputs for LCA for this thesis are trip range, trip fuel mass, engine mass, cruise altitude, flight time and number of flights from the preliminary sizing of the aircraft. To understand how the flight parameters of an aircraft can be optimized to reduce the environmental impact, one should refer to Caers 2019.

5 Results

The results from the aircraft of all the concepts mentioned in chapter 4 are presented here. In both the tools i.e. PreSTo for propeller and turbofan engine driven aircraft, a baseline aircraft was created similar to A320. Using the baseline aircraft in both cases, the results are normalized in order to compare them with A320. In the following section, results from different types of turbo-electric/hydraulic propulsion systems are reviewed. A total of 8 configurations are analysed. The following nomenclature is used to classify aircraft configurations : the first two letter indicate the type of gas turbine engine used (turboshaft (TS) or turboprop (TP)), the third and fourth letter describe the type of propulsion architecture used (turbo-electric (TE) or turbo-hydraulic (TH)) and number presents the number of propulsors used.

5.1 Turbo-Electric/Hydraulic Propulsion System

5.1.1 Mass Breakdown of Propulsion System

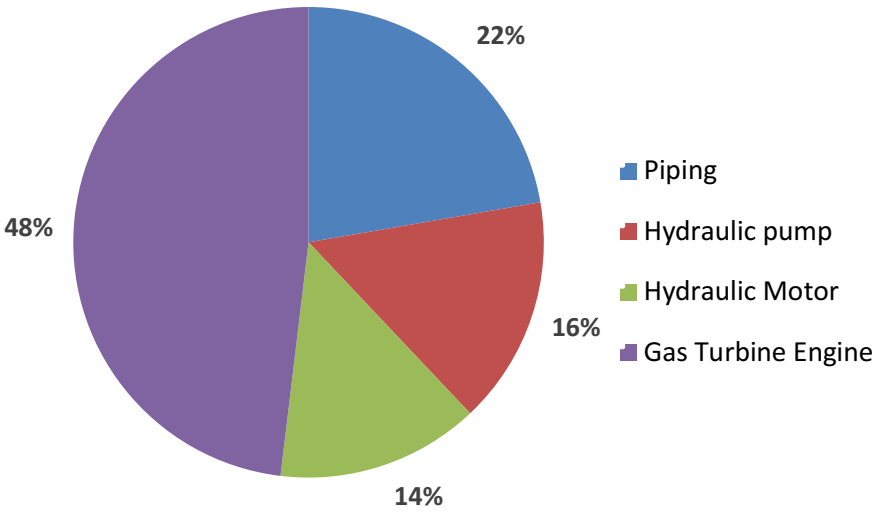

Figure 5.1 Mass breakdown of turbo-hydraulic propulsion system

Figure 5.1 shows the breakdown in mass of the turbo-hydraulic propulsion system. The gas turbine engine occupies majority of the pie since it produces the majority power required and it also compensates for the inefficiencies of the overall system. The piping for the hydraulic fluid is heavy because it includes the mass of the fluid, pressure line pipe and return line pipe. Also, the many of the small components such as valves and filters are not taken into account.

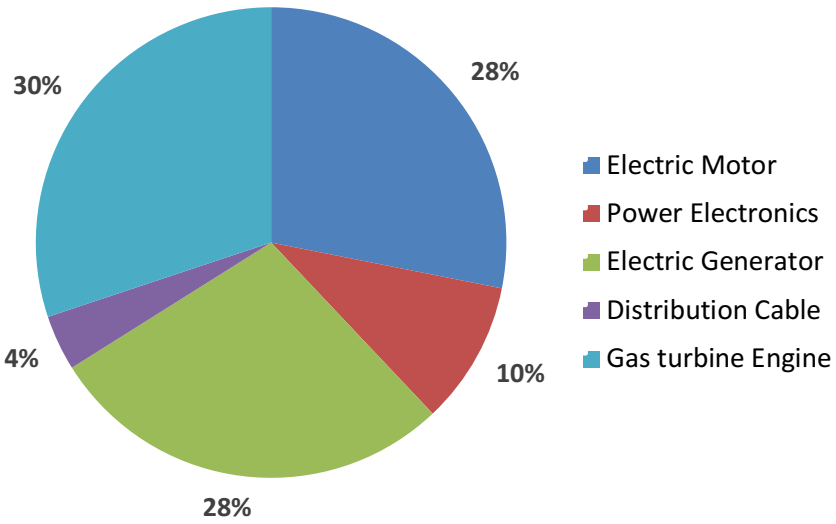

Figure 5.2 Mass breakdown of turbo-electric propulsion system

In Figure 5.2, one can notice the distribution of mass of the turbo-electric propulsion system. Similar to turbo-hydraulic system, the gas turbine engine is heavier than other components. The power electronics and distribution cable lighter but if the sizing the distribution cables might be heavier in reality.

5.1.2 Maintenance Costs

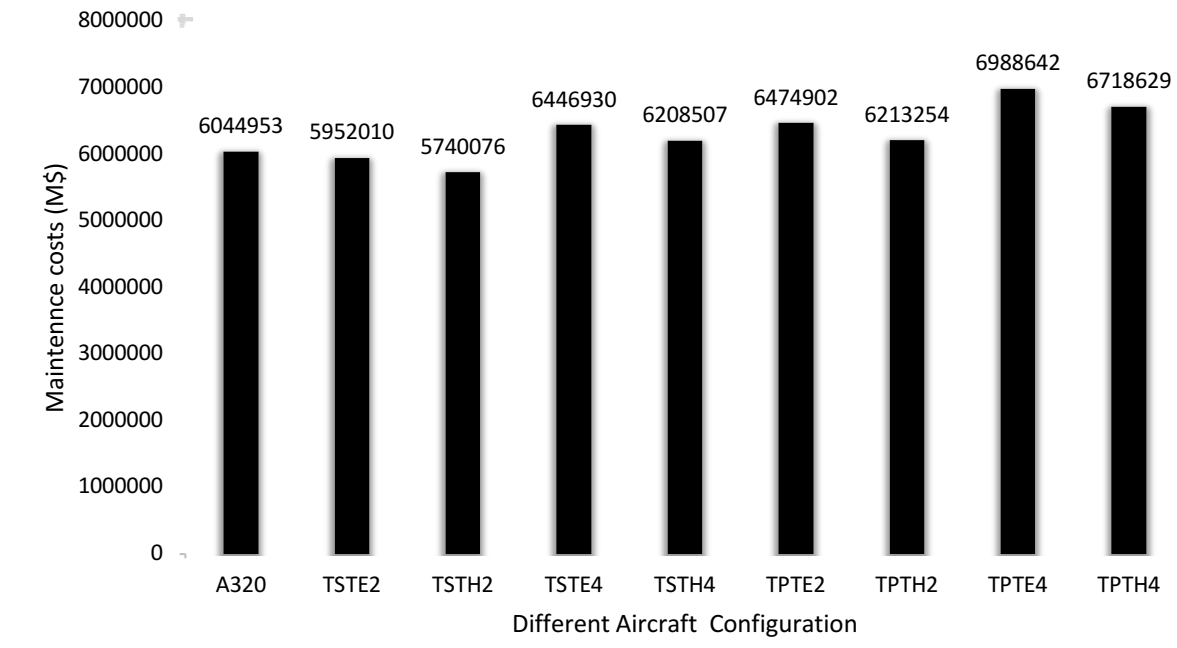

Figure 5.3 Different aircraft configurations vs maintenance costs

In Figure 5.3, the maintenance costs of studied aircraft configuration are represented. It is deduced that TSTH2 has the lowest maintenance cost, even smaller than A320. Another deduction is that, the maintenance costs increase with the number of engines and it seems appropriate. The turboprop engine equipped aircraft have higher costs due to its higher mass compared to turboshaft engines. The reduction in costs also arise from the lower number of shafts and compressors stages. Similarly, the electric engines have higher costs due to their high specific power.

In fact, the hydraulic system needs more maintenance. According to Rosero (2006), the maintenance costs of electric system is lower than a hydraulic system. This specific difference cannot be taken into account in the AEA method for calculating DOC since in this method, the calculation of Maintenance Costs mainly relies on the operating empty mass of the aircraft. Also, according to Caldwell (2018), the price of hydraulic motors is less expensive.

5.1.3 Trip Fuel Mass & PSFC

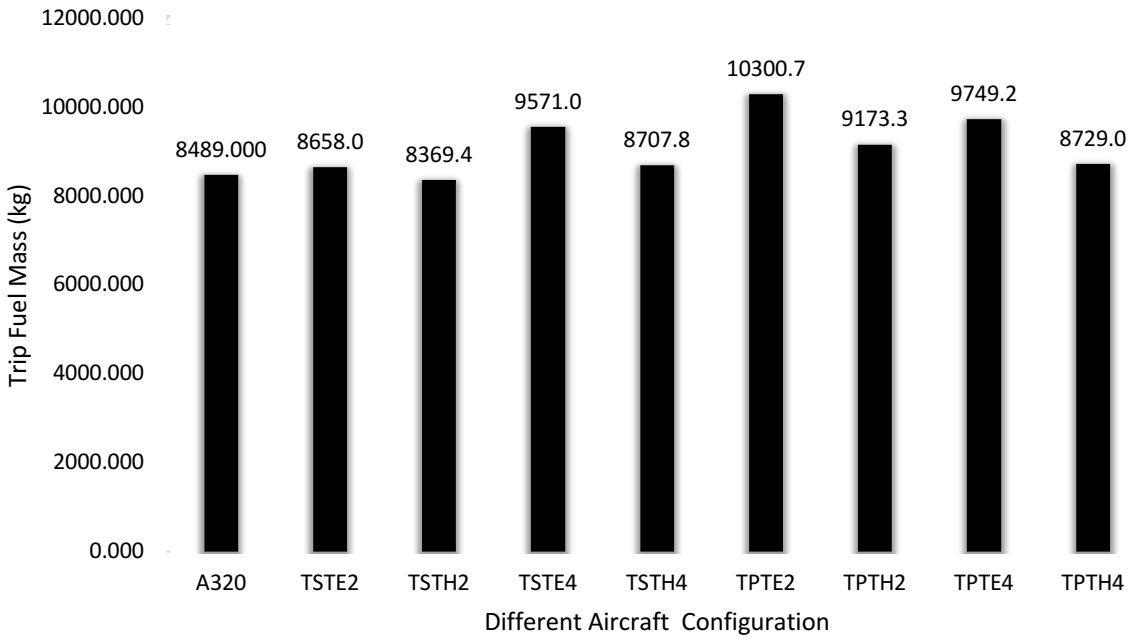

Figure 5.4 Different aircraft configurations vs trip fuel mass

The above graph provides an interesting outlook on the variation in trip fuel mass for different aircraft configuration. Repeatedly, the fuel mass of TSTH2 is the lowest. It is mainly because of the lower PSFC of turboshaft engine. The difference pattern in fuel mass due to number of engines varies according to the gas turbine engine.

The difference in pattern is mainly due to the Power specific fuel consumption (PSFC) of the gas turbine engines. The PSFC of turboshaft was calculated based on the requirement of power for every specific aircraft while for turboprop engine a standard PSFC was applied.

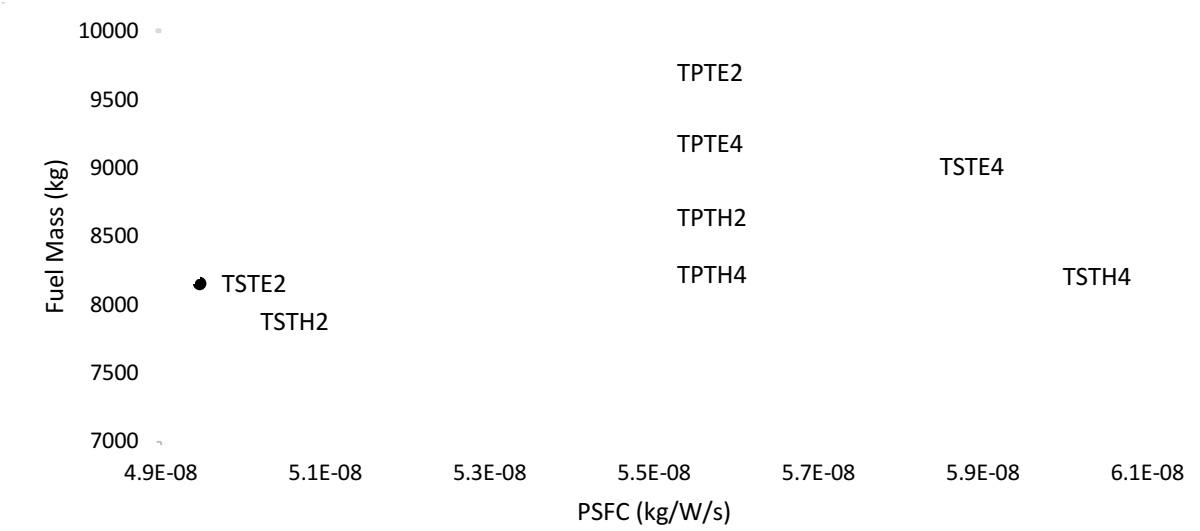

Figure 5.5 PSFC vs fuel mass

For turboprop engine, increasing the number of engines decreases the fuel required. This difference is because of the increase in propeller efficiency during cruise, landing, take-off and second segment climb. Since the power required for take-off by one engine is lower for a 4-engine aircraft, the PSFC is higher. Therefore, for turboshaft engine, the PSFC increases with the decrease in power required and hence the power required is inversely proportional to fuel mass.

5.1.4 Propeller Efficiency

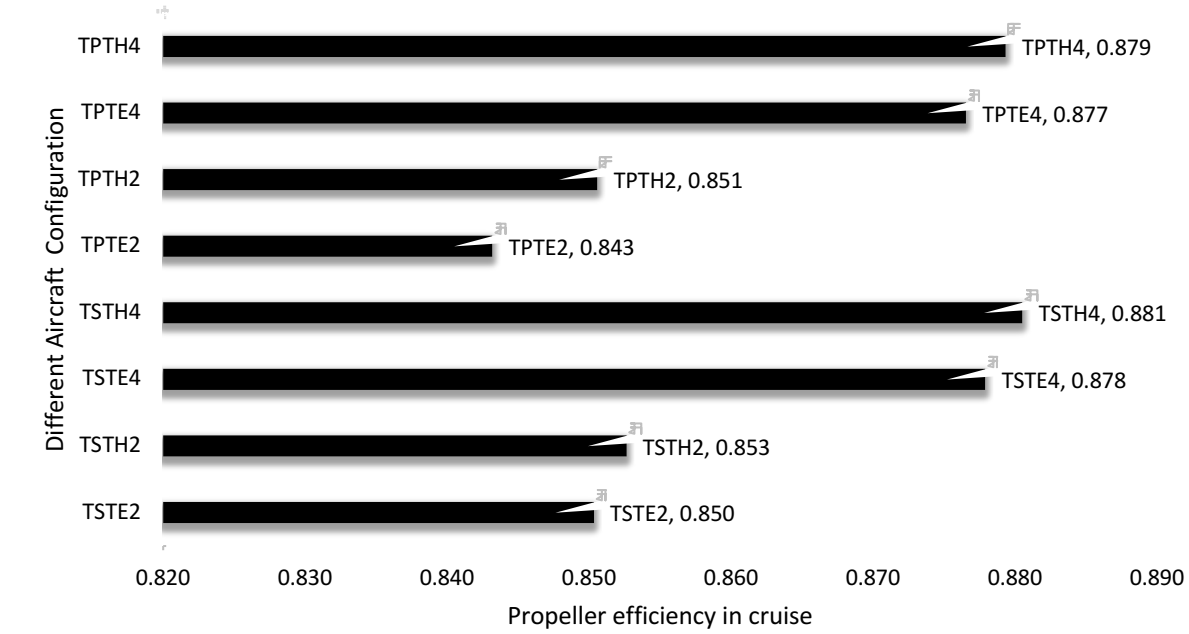

Figure 5.6 Different aircraft configurations vs propeller efficiency in cruise

In Figure 5.6 the variation in propeller efficiency in cruise is studied. It is visible that when the number of engines increase, efficiency increases. This is because the disc loading decreases with the decrease in power required by one engine. Also, this graph is only ideal, considering the diameter of propeller is constant. The requirements such as ground clearance angle and gap between two engines along the wing must be fulfilled. However, one must not exceed the ICAO aerodrome reference codes for wingspan. Since A320 aircraft falls in the second category where the wingspan is limited to 36 m. Therefore, the maximum propeller diameter is equal to 7 m.

5.1.5 Distributed Propulsion System

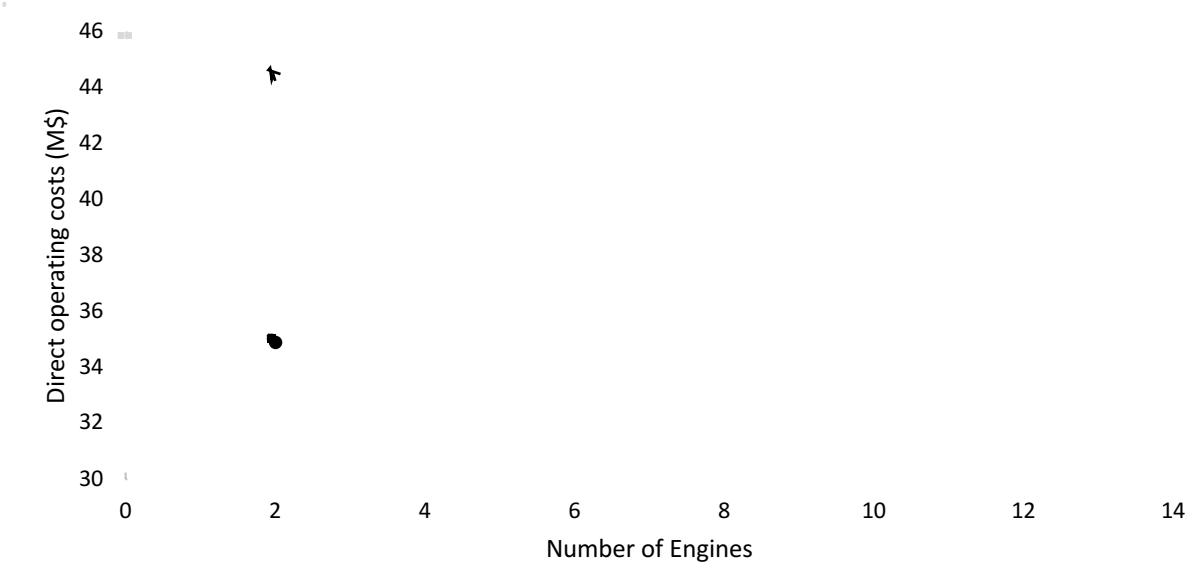

Figure 5.7 Number of engines against direct operating cost (M$)

Figure 5.7 represents the variation of direct operating costs with respect to change in number of engines. This graph was created to study the effects of distributed propulsion system on the conceptual aircraft. The TSTH aircraft was used for this calculation with constant $sin\gamma$. The propeller diameter was sized accordingly to fit in the 36 m wingspan. The SFC was assumed to be constant, since a single turboshaft engine will be able to power all the motors. Using the tool created for designing and deriving different aircraft concepts for turbo-hydraulic/electric propulsion, 6 new aircraft were designed. It is noticeable that increase in number of engines lead to higher DOC.

In Brüge 2018, a similar research was carried out in detail. In this research the maintenance costs of the aircraft were calculated with varying number of engines according to different cost calculation methods. Unlike present master thesis, the number of engines were increased without changing the overall aircraft design in Brüge 2018. It was found that the maintenance costs decrease when the number of engines is more than 3.

Table 5.1 Propeller diameter with increase in number of engines

Number of engines	Propeller diameter (m)
2	8.5
4	8
6	5
8	3.5
10	2.6
12	2

According to Kerho (2013), when the motors are ducted and placed at optimum locations on the wing, there are benefits from accelerating the airflow and from differential thrust. Albeit these concepts cannot be integrated in the aircraft tool used because of the complex CFD simulations required. It is evident that ducted fans reduce the propeller efficiency (Scholz 2018b) although it is argued otherwise. A possible reason is that the increases in number of engines can lead to increase operating empty mass because of the components required. Also, as shown in Figure 5.3, the maintenance costs increase.

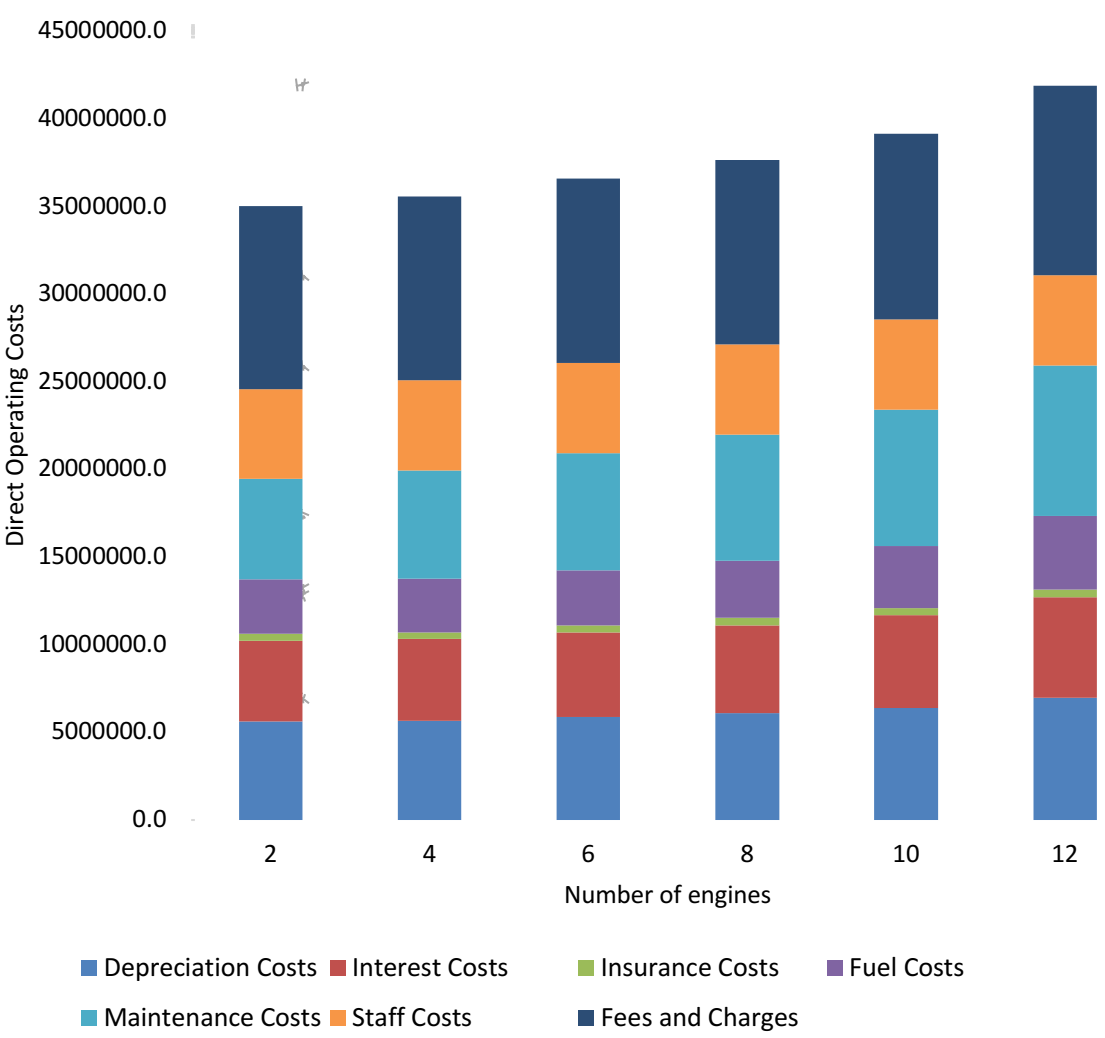

Figure 5.8 Various costs vs. Number of engines

In the above graph, a detailed comparison of different costs with increasing number of engines are plotted. One can see large increases in Depreciation and Maintenance costs. The maintenance costs mainly rely on the mass and number of engines. In this case, even though the mass of a single motor reduces, the number of motors increase and also number of components. The operating empty mass of the aircraft increases as a result of snowball effect. Although, the mass of the wing might reduce due to increase in number of engines since it decreases wing bending.

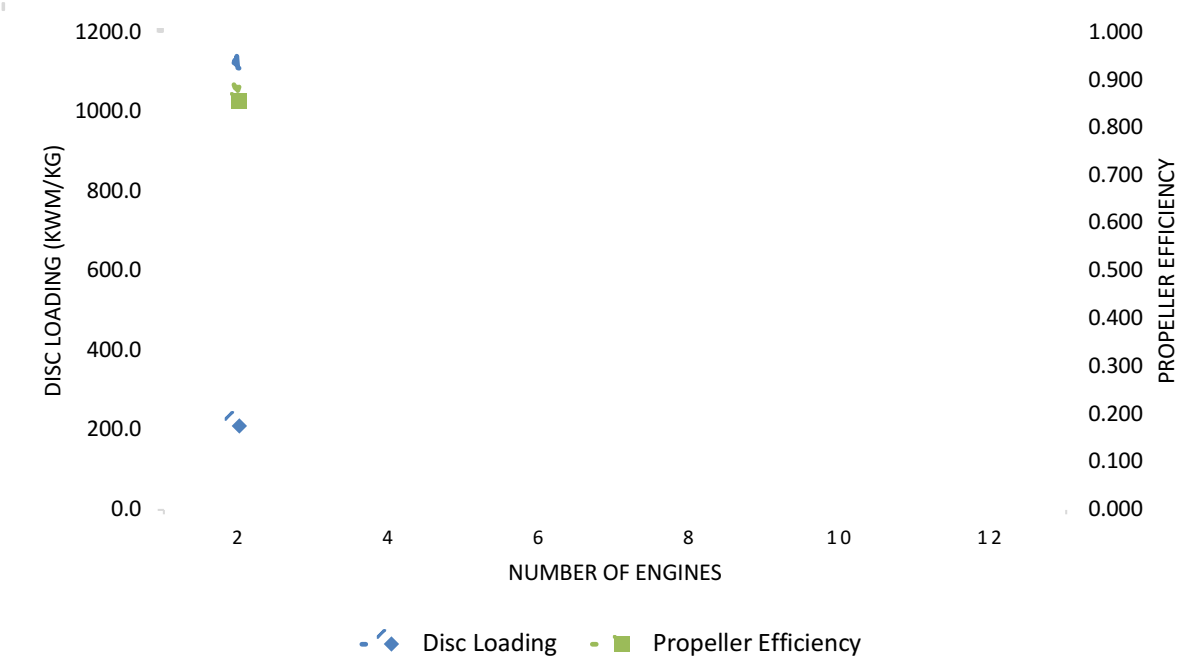

Figure 5.9 Comparison of disc loading and propeller efficiency with number of engines

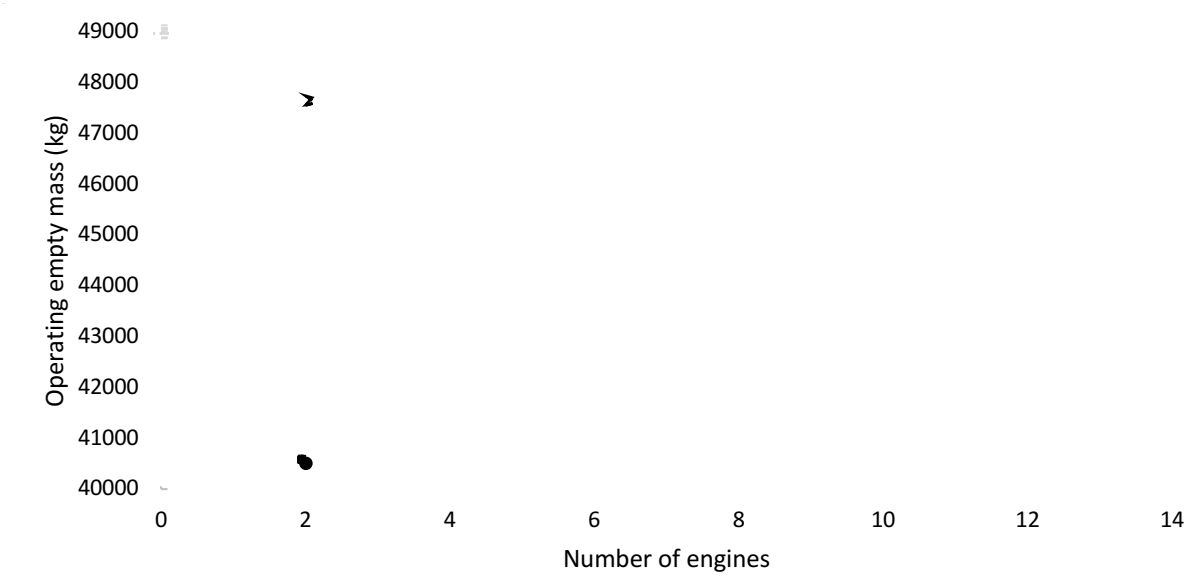

Figure 5.10 Variation of operating empty mass with increasing number of engines

In Figure 5.9, the propeller efficiency in cruise is compared with the increasing number of engines and aircraft model with 4 engines has the highest. The reason for this could be because of the lower disc loading, also represented in the Figure 5.9. The disc loading mainly depends on the power required, which in turn depends on the mass of the aircraft. From Figure 5.10, it also evident that the snowball effect for operating mass of the aircraft increases rapidly. The reason for the lower disc loading for the 4-engine aircraft is from the lower operating mass which is almost equal to 2-engine aircraft.

5.1.6 Direct Operating Costs

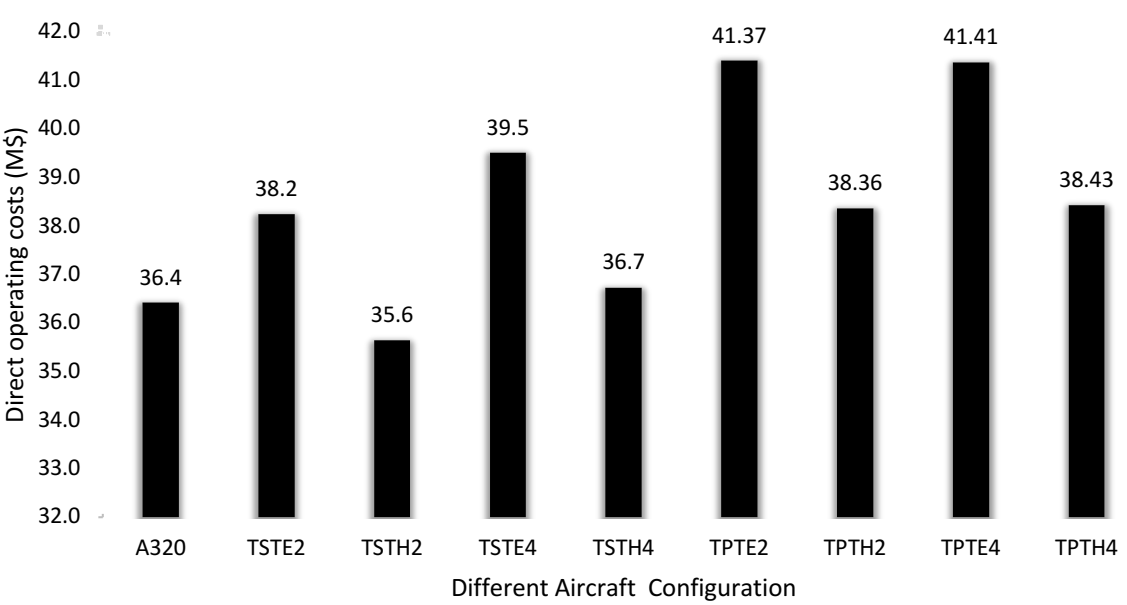

Figure 5.11 Different aircraft configurations vs direct operating costs (M$)

A diverse set of parameters from aircraft design, influence the operating costs of an aircraft. From the graph, one can deduce that DOC increases with the number of engines. Also, TSTH2 aircraft has a lower DOC compared to A320 due to lower mass of engines and fuel consumption. A major drawback with all the proposed aircraft configurations, is that it is assumed that gas turbine engines are housed in the cargo compartment. This might initially lead to lack of cargo space and reduce revenue.

5.1.7 Overall Comparison

In the Table 5.2, the important parameter for evaluating an aircraft is given with the deviation from the A320 model. While comparing all the parameters, TSTH2 is the best option. As discussed before. The operating empty mass of TSTH4 is lower than A320. This means that the collective mass of 4 engines are less than the mass of two turbofan engines mainly due to the lower power requirement from each engine.

The TSTH4, mainly satisfies the criteria by having the same number of flights per, flight and cruise speed. Since reduction in $n_{t,a}$ can lead to reduction in revenue for aircraft operator or the airline. The result of the propeller driven aircraft is better than A320 due to the increase in bypass ratio. By installing one core engine, in this case the turboshaft engine, a propeller driven by a motor has a higher bypass ratio compared to a turbofan engine.

Table 5.2 Comparison of aircraft parameters and different aircraft configurations

	TSTE2	**TSTH2**	**TSTE4**	**TSTH4**	**TPTE2**	**TPTH2**	**TPTE4**	**TPTH4**
m_E	+76%	-8%	-10%	-54%	+153%	+60%	+15%	-30%
m_{OE}	+14%	+8%	+15%	-1%	+29%	+11%	+24%	+8%
m_{MTO}	+9%	-2%	+11%	0%	+21%	+8%	+17%	+5%
S_W	+8%	-3%	+10%	-1%	+20%	+7%	+16%	+4%
V_{CR}	0%	0%	+1%	+1%	-1%	0%	+1%	+1%
H_{CR}	-4%	-5%	-12%	-13%	-3%	-4%	-12%	-13%
DOC	+5%	-2%	+8%	+1%	+14%	+8%	+15%	+6%
$n_{t,a}$	0%	0%	+1%	+1%	0%	0%	+1%	+1%
t_f	0%	0%	-1%	-1%	0%	0%	-1%	-1%

Table 5.3 Comparison of CO_2 and Single score different aircraft configurations

	CO_2 in Cruise (g/PKM)	**CO_2 SS**	**SS**
TSTE2	+2%	+2%	+8%
TSTH2	-7%	-7%	-1%
TSTE4	+13%	+12%	+20%
TSTH4	+8%	+7%	+14%
TPTE2	+22%	+21%	+28%
TPTH2	+2%	+2%	+8%
TPTE4	+15%	+14%	+23%
TPTH4	-3%	-2%	+3%

In Table 5.3, results from the LCA are represented as deviations from A320. In the 8 models compared here, only two models have lower CO_2 emissions compared to A320 aircraft. However, the single score (SS) of the TPTH4 aircraft is 3% more than A320 because of the increase in operating empty mass that leads to increase in materials required and their environmental impact. TSTH2 is observed to be the best candidate in this propulsion system architecture.

5.2 Partial Turbo-Hydraulic/Electric Propulsion System

5.2.1 Engine Mass

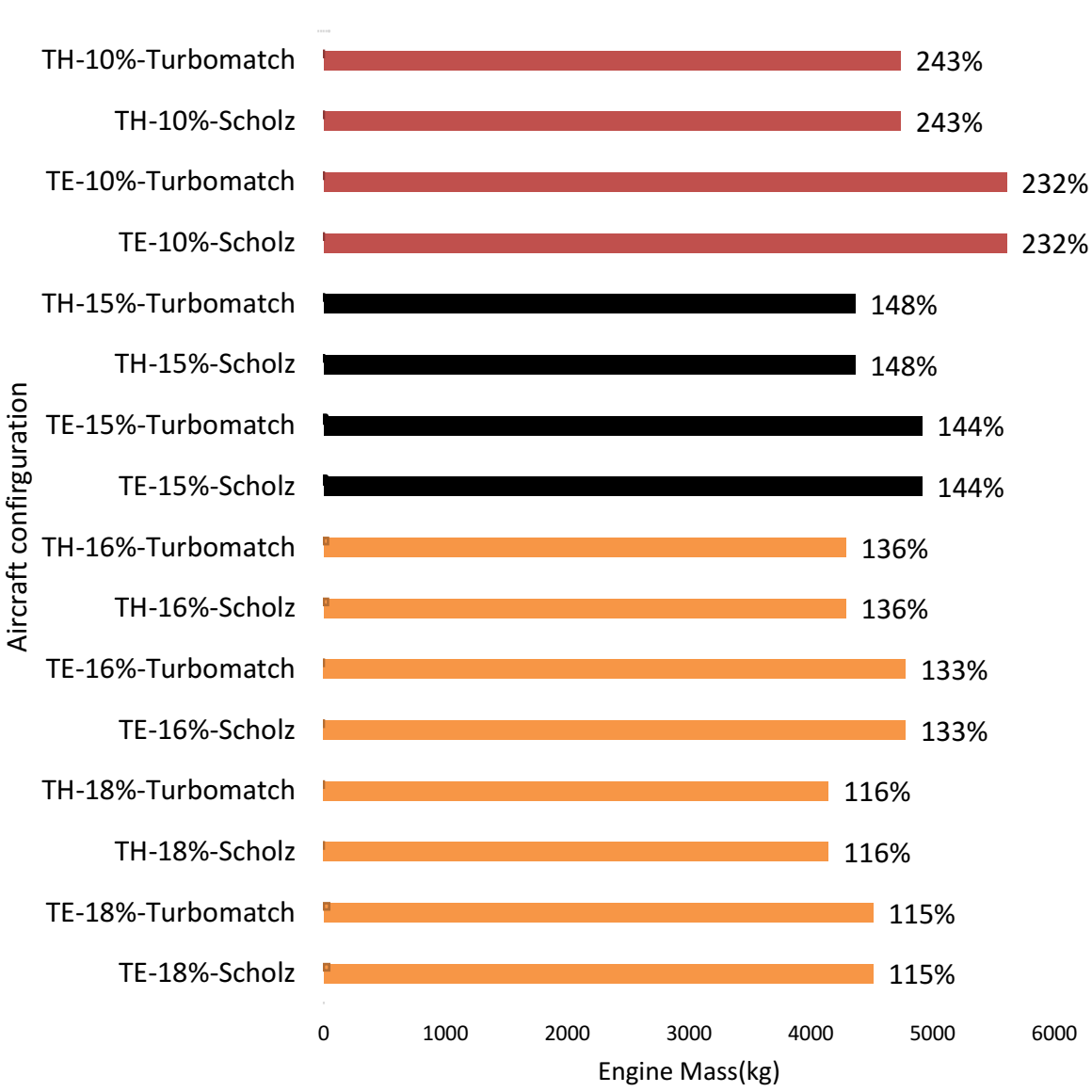

Figure 5.12 Total engine mass & engine operation % vs aircraft configuration

The partial turbo-hydraulic/electric propulsion concept was studied by implementing these propulsion architectures in an aircraft with the requirements of A320 aircraft. In Figure 5.12, the total mass of the propulsion system is plotted against the various aircraft configurations. As mentioned previously the TH and TE are abbreviations for Turbo-hydraulic and Turbo-electric propulsion system. The values of percentages from 10% to 18% is the amount of thrust produced by the turbofan engine of the take-off thrust. The two types of methods to determine kp, are named as Scholz and Turbomatch.

The turbofan engine operation % is also mentioned beside every aircraft concept. The turbofan engine operation % should be less than 140% in order to observe a realistic view with the existing technology. Therefore, in the above graph, the bars in red indicate that, it is above the required operation %. The black bars represent that the aircraft are slightly above the required level and orange bars indicate that the aircraft are within the requirement.

Observing the Figure 5.12, one can deduce that turbo-hydraulic engines generally weight less than turbo-electric engines. However, the turbo-electric engines have a reduced operation % compared to alternate option. This is the result of high efficiency of the electric motor and components. Although, operation % of turbofan and engine mass of both the kp methods are equal with equal thrust levels, the TSFC of the aircraft differ. This will be explained further in this chapter. One can deduce that with the decrease in thrust level, the mass of the propulsion systems increases. As the thrust produced by the turbofan engine decreases, the motor must provide the remaining required thrust. If the thrust produced by the motor increases, it also required to size the motor and its components according to the lager requirement. Thus, decreasing the thrust produced by the turbofan engine increase the mass of the overall propulsion system. Figure 5.13 compares the mass breakdown of the complete propulsion system.

The pie chart on the left represents the composition when thrust level is 10% as opposed to 18% on the right. This comparison was made for partial turbo-hydraulic propulsion system. It is evident that contribution of mass for motor and its components decrease from 27% to 7%. However, the total mass of the propulsion system slightly decreases between the two figures.

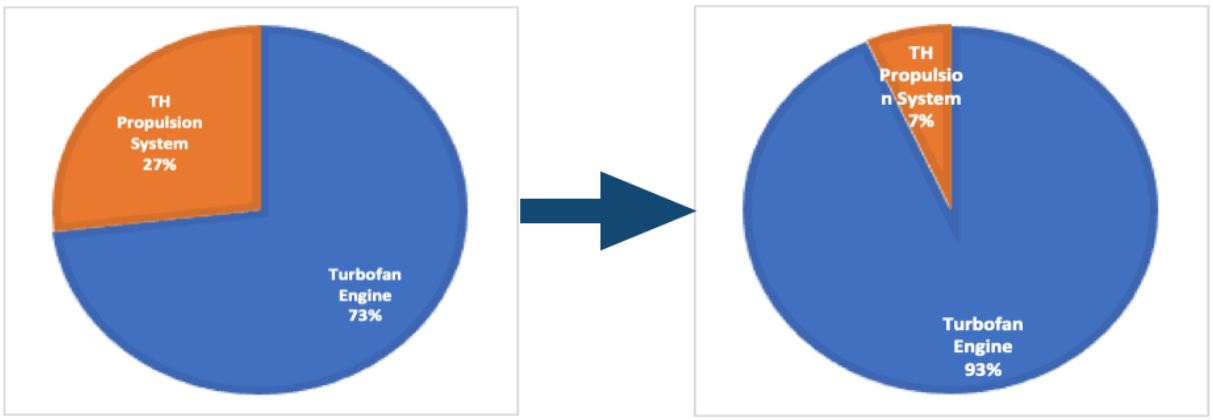

Figure 5.13 Comparison of propulsion systems for thrust levels of 10% and 18%

5.2.2 Fuel Mass

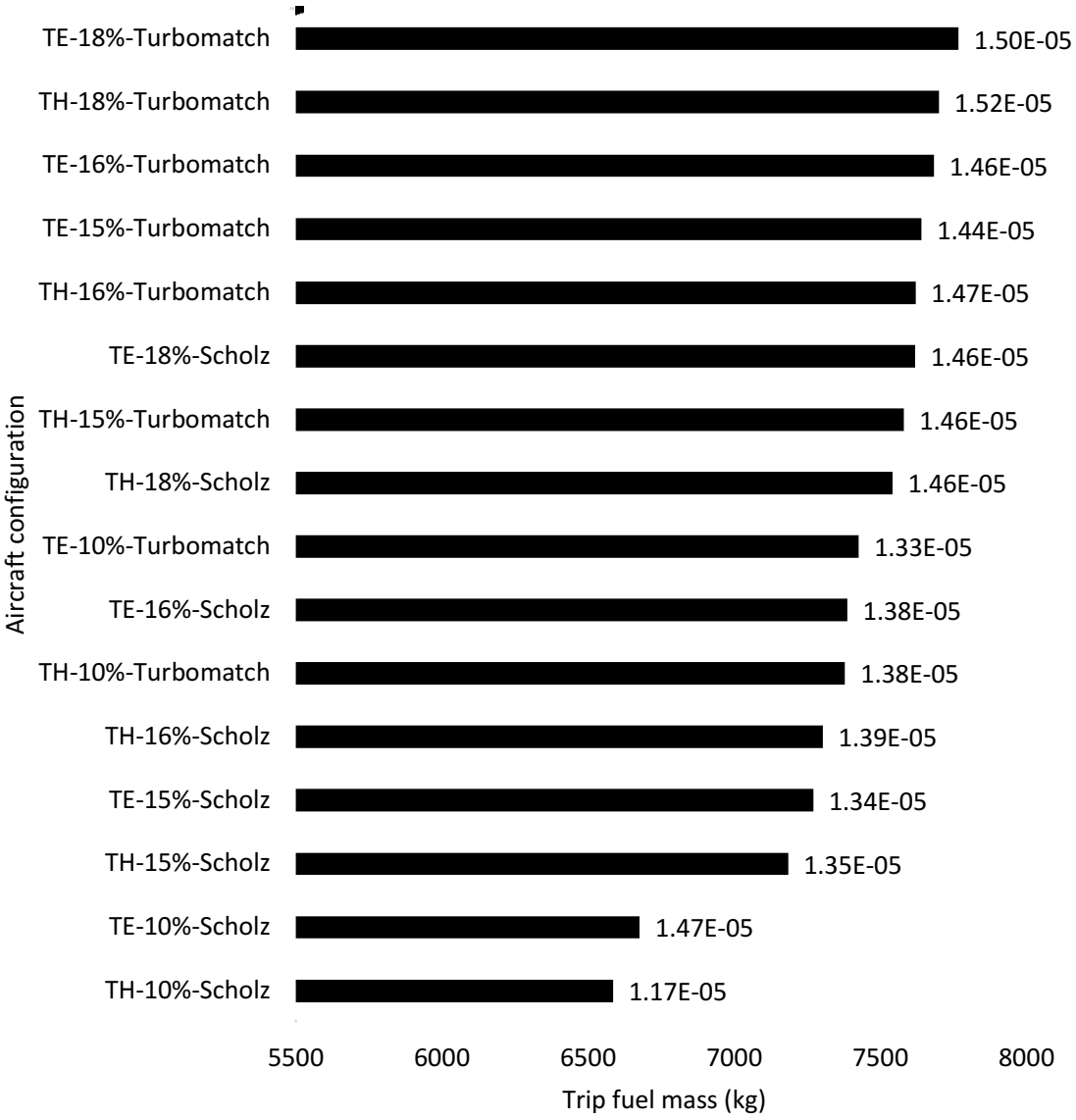

Figure 5.14 Trip fuel mass(kg) & TSFC (kg/W/s) vs aircraft configuration

In the above graph, trip fuel mass is plotted against the different aircraft configurations. Also, the new TSFC found for each aircraft is mentioned next to the bar. In the previous section, where the total engine masses were analysed, it was found that the engine mass decreases with the decrease in thrust produced by the motor. However, for trip fuel mass, it is evident that as that the motor produces higher amount of thrust, the TSFC and trip fuel mass decrease. The deduction of decrease in TSFC and trip fuel mass can be explained by reasoning that the shaft off-take power consumes less fuel. Hence, when the motor utilizes the shaft off-take power for producing thrust, TSFC reduces with increase in contribution to cruise thrust. According to Figure 5.14, propulsion system where 10% of the take-off thrust is produced by turbofan engines, consume less fuel. The practicality of this theory can be questioned by integrating the engine operation % which more than 200% for the mentioned propulsion system.

5.2.3 Overall Comparison

Table 5.4 Comparison of aircraft parameters and different aircraft configurations

	m_F	DOC	TSFC	T_{TO}/n_E	m_{OE}	m_{MTO}
TH-10%-Scholz	-15%	0%	-24%	+3%	+4%	+3%
TH-15%-Scholz	-7%	0%	-12%	+1%	+2%	+2%
TH-16%-Scholz	-6%	0%	-10%	+1%	+2%	+1%
TH-18%-Scholz	-3%	0%	-5%	+1%	+1%	+1%
TH-18%-Turbomatch	-1%	0%	-2%	+1%	+1%	+1%
TH-16%-Turbomatch	-2%	+1%	-5%	+1%	+2%	+2%
TH-15%-Turbomatch	-2%	+1%	-5%	+1%	+2%	+2%
TE-18%-Scholz	-2%	+1%	-5%	+2%	+3%	+2%
TH-10%-Turbomatch	-5%	+1%	-10%	+3%	+4%	+3%
TE-16%-Scholz	-5%	+1%	-10%	+3%	+4%	+3%
TE-18%-Turbomatch	0%	+1%	-3%	+2%	+3%	+2%
TE-15%-Scholz	-6%	+1%	-13%	+3%	+5%	+4%
TE-16%-Turbomatch	-1%	+2%	-5%	+3%	+4%	+3%
TE-10%-Scholz	-14%	+2%	-26%	+6%	+8%	+6%
TE-15%-Turbomatch	-1%	+2%	-7%	+3%	+5%	+4%
TE-10%-Turbomatch	-4%	+3%	-13%	+6%	+8%	+6%

Table 5.6 provides a detailed comparison of all the aircraft analysed for partial turbo-electric/hydraulic propulsion system with A320 aircraft. The comparison is given in % of deviation from the values of the reference aircraft. The main parameters used to identify the best candidate are fuel burn and DOC as they align with objectives of this research. From the previous sections it is noticeable that TH/TE-10% aircraft have a lower fuel mass, but they cannot be considered due to their turbofan engine operation %. When comparing the inefficiency of TH/TE-18% and improbability of TH/TE-10%, TH/TE-15% & 16% are observed to be good candidates. However, from Figure 5.12, TH/TE-15% is also eliminated. Therefore TH/TE-16% can be considered as ideal candidates and specifically TH-16%-Scholz can be chosen as the best candidate. TH-16%-Scholz is 2% more heavier than A320 in terms of operating empty mass but reduces the TSFC by 10%. The benefits of TH are already mentioned in the previous sections. The accuracy of Scholz method can be questioned

5.2.4 Life Cycle Assessment

Table 5.5 Comparison of CO_2 and Single score for different aircraft configurations

	CO_2 in Cruise (g/PKM)	**CO_2 SS**	**SS**
TH-10%-Scholz	-23%	-22%	-20%
TH-15%-Scholz	-16%	-15%	-12%
TH-16%-Scholz	-15%	-13%	-11%
TH-18%-Scholz	-12%	-11%	-8%
TH-18%-Turbomatch	-10%	-9%	-6%
TH-16%-Turbomatch	-11%	-10%	-7%
TH-15%-Turbomatch	-11%	-10%	-7%
TE-18%-Scholz	-11%	-10%	-7%
TH-10%-Turbomatch	-14%	-13%	-10%
TE-16%-Scholz	-14%	-12%	-10%
TE-18%-Turbomatch	-9%	-8%	-5%
TE-15%-Scholz	-15%	-14%	-11%
TE-16%-Turbomatch	-10%	-9%	-6%
TE-10%-Scholz	-22%	-21%	-18%
TE-15%-Turbomatch	-10%	-10%	-7%
TE-10%-Turbomatch	-13%	-12%	-9%

The Table 5.5 is comparison all the aircraft configuration and their environmental impact in terms of deviation from A320 aircraft. While comparing Scholz and Turbomatch method, Scholz method shows a reduction in environmental impact. It is also evident that all the aircraft configurations have less emissions and SS with respect to A320. TH-10%-Scholz, makes the least environmental impact and TE-18%-Turbomatch makes the most among the partial turbo-electric/hydraulic propulsion systems. As previously chosen, TH-16%-Scholz is relatively in the midpoint of these values.

6 Discussion

6.1 Comparison of Most Advantageous Propulsion Systems

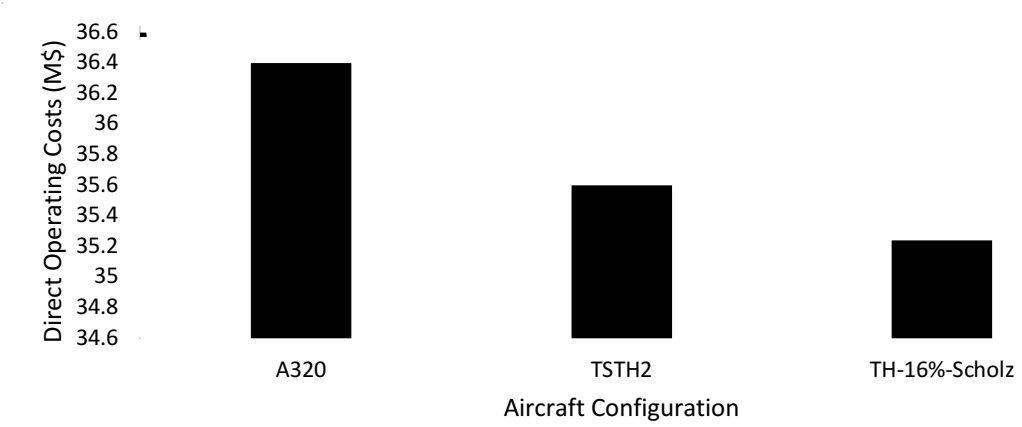

Figure 6.1 Comparison of DOC of superior propulsion systems with A320

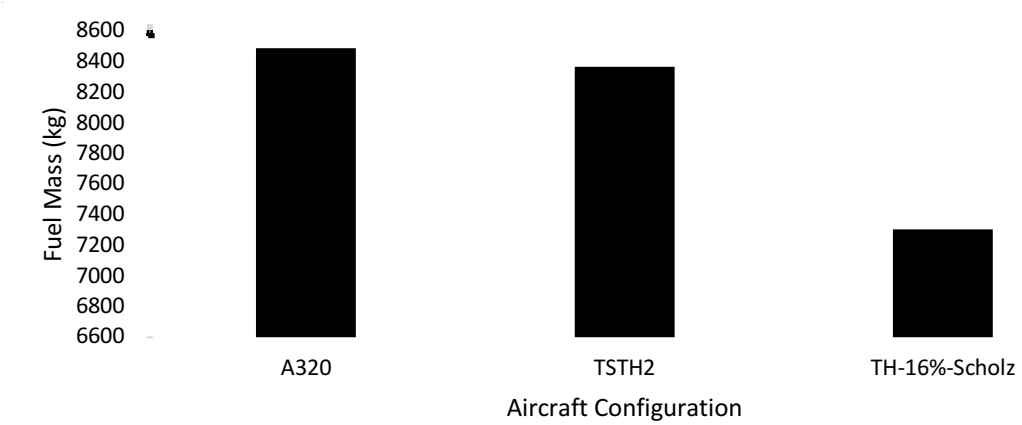

Figure 6.2 Comparison of fuel mass of superior propulsion systems with A320

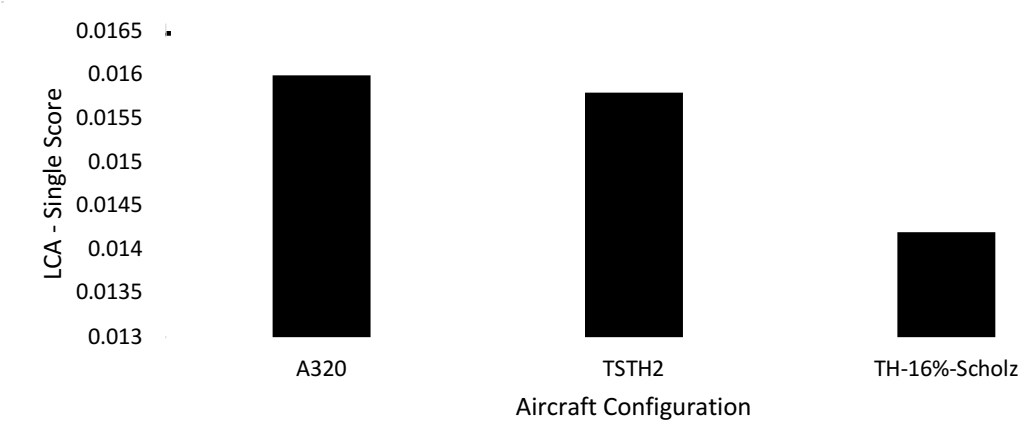

Figure 6.3 Comparison of LCA of superior propulsion systems with A320

In the previous chapter, the results from aircraft design of all the propulsion concepts were presented. In this section, the best aircraft from each propulsion system concept is compared with the reference aircraft A320. Figure 6.1, 6.2 and 6.3 compare these aircraft in terms of DOC, fuel mass and LCA to fulfil the objective of this research. One apparent observation from the figures is that partial turbo-hydraulic propulsion system is superior to turbo-electric/hydraulic and classic jet propulsion.

A few requisites have to be stated before comparing the three aircraft. Turbo-hydraulic system is superior in fuel burn, DOC and LCA to turbo-electric propulsion because both the novel concepts chosen for comparison are equipped with only turbo-hydraulic system. TSTH2 aircraft is only slightly better than A320. Since this a conceptual design, there many factors are not considered and have been ignored. These factors might increase the overall mass and thus the DOC and LCA. It would only be worth to proceed with the detailed research if the design proves to have significant advantages. Having this perspective, TH-16%-Scholz seems to have the advantage over the latter.

The LCA analysis was based mainly on the engine mass, operating empty mass and fuel burn. But other factors such as materials used for electric system and hydraulic systems were not analysed. Furthermore, having more engines lead to more basic components and can lead to further damage to the environment. Therefore, a detailed analysis can lead to disadvantage for the researched propulsion system concepts.

6.2 Benefits and Drawbacks of Researched Propulsion Concepts

For TSTH2, 100% of the shaft power is extracted to drive the generators/pumps and the gas turbine itself does not produce any thrust. The advantage that the turbofan engine gains is by producing thrust while also supplying power to the motors. Thus, increases the bypass ratio of the engine. TSTH2 also increases the bypass ratio by having single core engine and many motors. While comparing these two concepts with A320 aircraft, the maximization of turbofan is limited by its size and cowling.

The advantages of being able to install the electric/hydraulic motors flexibly is unprecedented. This advantage is applicable for both the propulsion concept. The fans can be placed at the most optimum position for gaining aerodynamic benefits by producing power at a different location for partially and completely turboelectric/hydraulic propulsion system. The main gas turbine engine can be located at a convenient location to receive undisturbed flow. While the fans can be located to ingest boundary layer and to reduce drag. Also, the fan speed and the shaft speed are decoupled. The electric or the hydraulic system act as a variable gearbox.

The partial turbo-electric/hydraulic configuration offers better access for maintenance, while completely turbo-electric/hydraulic system with embedded engines can cause difficulty during maintenance.

Also, the heat produced by the engine must be dissipated efficiently. Heat insulation techniques and exhaust for engines can be adapted from fighter aircraft that are installed with engines inside the fuselage. Although, it might need additional insulation material that can increase the operating empty mass. As a snowball effect, it will lead to increase in DOC.

Table 6.1 Noise level data of A400M and A320 aircraft (EASA 2019)

Aircraft Name	Full Power EPNdB	Flyover EPNdB	Approach EPNdB
Airbus 400M	95.6	90.6	102.5
Airbus 320-200	93.4	85.8	95.5
Airbus 350-900	90	87.9	96.4

The industry is currently pushing towards quieter flights and installing gas turbine engines inside the fuselage does not support a quiet flight. Table 5.3 is a comparison between aircraft with the noise level in effective perceived noise in decibels (EPNdB). The A320 aircraft is compared with A400M and A350-900. A400M was chosen for comparison because its design characteristics are similar to the aircraft proposed.

Currently, A350 aircraft is said to have the quietest cabin according to BDL (2019). It is evident that propeller driven aircraft have a higher noise level compared to jet propelled aircraft (EASA 2019). It should be noted that, A400M is a defence cargo aircraft and the noise insulation for the cabin will be minimum. It is also evident that A350-900 consists of a quiet cabin because of the noise insulation used for the cabin. A massive insultation will be required for the proposed aircraft, since the engines are placed inside the fuselage.

The propellers driven by the motors cannot perform well at high altitudes where the turbofan engines typically fly. The turbofan engines fly in high altitude due to the reduction of density and better efficiency. In order to fly at high altitudes, the aircraft will have to travel at high velocity. Flying at high velocity for propellers can lead to increase in drag due to high blade tip speed. Therefore, for a turbofan engine and a propeller driven by a motor cannot work efficiently at a specific altitude.

Although hydraulic system is proven earlier to be superior to electric system, it would be advantageous to use the latter. Since the cabin and the inflight equipments are powered by electric system, a large power-offtake for electric system can decrease the mass of additional components.

6.3 Future Work

When the complete design of the partial turbo-hydraulic propulsion system is proven, the shaft off-take power extraction of the turbofan engine can be improved by designing the core and turbine specially to meet the requirements. Many more thrust levels can be efficient and become reality. In Figure 6.4, max rated horse power extraction as % of shaft power is compared for different engines. It also shows that latest generation engines extract more % of shaft power. The increase in extraction of shaft power is because all the manufacturers head towards a more electric aircraft.

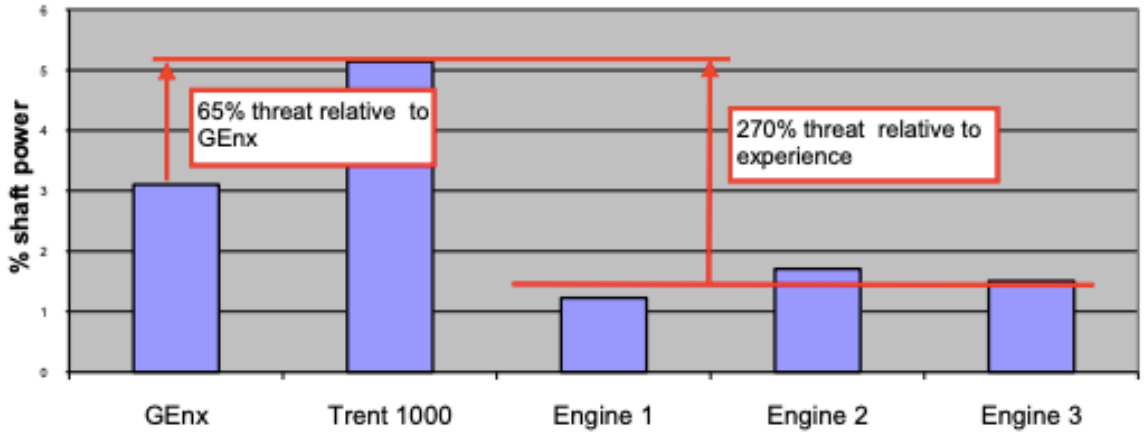

Figure 6.4 Shaft Power offtake levels of different turbofan engines (Lupelli 2011)

The overall mass of the electric system is said to be diminished in the future by manufacturing components with superconductive materials as shown in Table 6.2. Even though the values in the below table look futuristic, NASA estimates to achieve this by 2030 (Smith 2018). This might lead to better aircraft design and efficiency. But comparing the two-propulsion system's mass breakdown in the current scenario, one can deduce that the electric system is heavier. Even though, the electric system is more efficient, the hydraulic system's power to weight ratio is lower.

Table 6.2 Superconductive components of electric system (Pornet 2017)

Component	Specific weight	Efficiency
Superconductive Motor	20 kW/kg	99%
Superconductive Cables	9.2 kg/m	100%
Power Electronics	18 kW/kg	99.5%
Generator	5 kW/kg	95%

Figure 6.5 A graphic mock-up of Airbus E-fan X (Airbus 2017)

A relatively new technology, the electric hybrid propulsion system is currently being tested on BAe 146. For further details about the Hybrid-Electric Bae146, please refer to Jayme 2019. Among the four gas turbine engines of the aircraft, one engine is replaced with a electric ducted fan (green engine in the Figure 6.5). Similarly, to demonstrate the partial turbo-electric/ hydraulic propulsion technology, the propulsion system can be integrated with the current A320 aircraft. After understanding the viability of the technology, it can be further researched, and a new aircraft can be designed to extract maximum benefits of this technology.

7 Conclusion

This paper provides an overview of turbo-electric/hydraulic, partial turbo-electric/hydraulic and distributed propulsion system. It mainly examined the decoupling of power generation device and thrust generation device. The quest to find the superior propulsion system model was fulfilled by creating and investigating the effectiveness of all the propulsion systems. The integration of novel propulsion systems into an existing commercial aircraft helped in understanding the viability of the concepts. The advantages of these technologies were tested based on their direct operating costs, environmental impact and fuel burn. The tools that were required to perform these examinations were developed by HAW Hamburg and modified according to the requirements of the thesis.

A simple mass model for turbo-hydraulic/electric system was developed initially and a total of eight aircraft were compared. The performance of this propulsion system was investigated by enabling them with turboshaft and turboprop engines. It was found that turboshaft engines were preferred compared to turboprop due to their fuel efficiency. During the analysis, it was determined that turbo-hydraulic propulsion system is superior to electric propulsion. The overall performance of the A320 aircraft was slightly overpowered by a turbo-hydraulic aircraft with two engines. Since the gas turbine engine in this model does not produce any thrust among many disadvantages that were discovered, an advanced hybrid model was developed.

In order to understand the performance of distributed propulsion, a specific aircraft was selected, and the number of engines were increased from 2 to 12 and investigated. During the study, the increase in number of engines demonstrated an increment in DOC. The fluctuations in propeller efficiency and disc loading were also examined.

The partial turbo-electric/hydraulic propulsion system was analysed having a turbofan engine to power the fans using shaft off-take power and produce thrust simultaneously. Scholz and Turbomatch methods were used to determine the revised TSFC that will recalculate the DOC for that aircraft. Different thrust levels were set up to investigate the change in performance by using different combinations. A total of 16 models were analysed and compared. Partial turbo-hydraulic concept demotes the performances of A320 and completely turbo-hydraulic concepts. This model for propulsion leads back to jet fuel but it is an initiative towards greener aircraft for the future.

Future research can be carried out by implementing a detailed calculation by including the aerodynamics advantages that can be extracted from this concept. An advanced superconducting material can be used for electric system and components to increase the efficiency to up to a 100%. The core engine of the turbofan engine can be sized accordingly in order to the maximize the overall efficiency.

List of References

ADVISORY COUNCIL for AVIATION RESEARCH and INNOVATION in EUROPE (ACARE), 2017. *Strategic Research and Innovation Agenda*, vol.1, p. 14. Available at: https://bit.ly/2Kuufh4, archived as: https://perma.cc/4DWG-BL34

AIGNER, B, NOLLMAN, M, STUMPF, E, 2018. *Design of a Hybrid Electric Propulsion System within a Preliminary Aircraft Design Software Environment*. Bonn: Deutsche Gesellschaft für Luft- und Raumfahrt - Lilienthal-Oberth. P.2. Available at: https://doi.org/10.25967/480153.

AIRBUS, 2017. *Airbus, Rolls-Royce, and Siemens team up for electric future Partnership launches E-fan X hybrid-electric flight demonstrator*. France : Airbus S.A.S. Available at: https://bit.ly/2vXjZpR, archived as: https://perma.cc/7ZRS-KXTY.

AIRBUS, 2019. *A320 Aircraft Characteristics – Airport and Maintenance Planning*. Blagnac Cedex, France : Airbus S.A.S. Available at: https://bit.ly/2IjsDUY, archived as: https://perma.cc/VZA9-PV8Q.

ANG, A W X, RAO, Gangoli, KANAKIS, T, LAMMEN, W, 2018. *Performance Analysis of an Electrically Assisted Propulsion system for a Short-Range Civil Aircraft*. Intitution of Mechanical Engineers, J Aerospace Engineering 2019, Vol. 233(4) 1490-1502. Sage Publications. Available at: https://journals.sagepub.com/doi/10.1177/0954410017754146.

ANTON, Frank, 2018. *Hybrid-Electric Propulsion Systems for Aircraft*. In: Electric and Hybrid Aerospace Symposium Cologne, 2018. UKIP Media and Events. Available at: https://www.ukintpress-conferences.com/uploads/SPEHAT18/d1_s1_p5_frank_anton.pdf, archived at: https://perma.cc/6RXE-YYT5.

BHASKAR, Roy, PRADEEP, A.M, 2012. *Lecture Notes - Jet Aircraft Propulsion*. Bombay, India: Indian Institute of Technology. P 23. Available at: https://nptel.ac.in/courses/101101002/downloads/Lect-27.pdf, archived as: https://perma.cc/P33N-L9ZM.

BRÜGE, Niklas, KRANICH, Felix, 2018. Wartungskosten von Passagierflugzeugen bei verscheidener Triebwerkanzahl berechnet nach DOC-Methoden. Hamburg: Project, Department of Automotive and Aeronautical Engineering, University of Applied Science of Hamburg. Available at: http://nbn-resolving.org/urn:nbn:de:gbv:18302-aero2018-04-30.011, archived as: http://doi.org/10.15488/4306.

BUNDESVERBAND DER DEUTSCHEN LUFTVERKEHRSWIRTSCHAFT, 2019. *Aircraft Noise. Berlin: German Aviation Association*. Available at: https://www.bdl.aero/en/topics-and-positions/sustainability/aircraft-noise/, archived as: https://perma.cc/2UCS-XSPR.

CAERS, Brecht. Conditions for Passenger Aircraft Minimum Fuel Consumption, Direct Operating Costs and Environmental Impact. Hamburg: Master Thesis, Department of Automotive and Aeronautical Engineering, University of Applied Science of Hamburg. Available at: http://library.ProfScholz.de .

CALDWELL, Niall, 2018. *Digital Displacement Technology for Aerospa*ce. In: Electric and Hybrid Aerospace Symposium Cologne, 2018. UKIP Media and Events. Available at: https://www.ukintpress-conferences.com/uploads/SPEHAT18/d1_s2_p4_niall_caldwell.pdf, archived as: https://perma.cc/ETQ4-5PDT.

COMPACT DYNAMICS, 2016. *Technology Examples – Aviation*. Starnberg, Germany: Compact Dynamics. Available at: https://www.compact-dynamics.de/en/aviation/, archived as: https://perma.cc/4AAH-QHY3.

CROCKNER, David, 2007. *Dictionary of Aviation – Second Edition*. London: A&C Black Publishers 2007. eISBN-13: 978-1-4081-0226-8.

EUROPEAN UNION AVIATION SAFETY AGENCY, 2019. *EASA Certification Noise Levels*. Available at: https://www.easa.europa.eu/sites/default/files/dfu/MAdB%20Heavy%20Prop%28190806%29.xlsx, archived as: https://perma.cc/UMK8-6MFW.

FELDER, James, BROWN, Gerald, DAEKIM, Hyun, CHU, Julio, 2011. *Turboelectric Distributed Propulsion in a Hybrid Wing Body Aircraft.* In: 20th International Society for Airbreathing Engines Gothenburg, 2011. Cleveland, USA: NASA Glenn Research Center. Available: https://ntrs.nasa.gov/search.jsp?R=20120000856.

GESSEL, Hendrik, WOLTERS, Florian PLOHR, 2018. *System Analysis of Turbo Electric and Hybrid Electric Propulsion Systems on a Regional Aircraft*. Belo Horizonte: International Council of the Aeronautical Sciences. Available at: https://bit.ly/2Mnen2f, archived as: https://perma.cc/KW3S-TEZX.

GUNSTON, Bill, 2009. *The Cambridge Aerospace Dictionary – Second Edition*. New York, USA: Cambridge University Press. Available at: https://bit.ly/2lKSaPe.

HATAMI, Houman, 2013. *Hydraulic Formulary*. Rexroth Bosch Group. Available at: https://www.boschrexroth.com/business_units/bri/de/downloads/hyd_formelsammlung_en.pdf, archived as: https://perma.cc/7ADB-TE7P

HÜNECKE, Klause, 2003. *Jet Engines – Fundamentals of Theory, Design and Operation*. Osceola, USA: Motorbooks International Publishers & Wholesalers, 1997. ISBN 0-7603-0459-9.

INTERNATIONAL AIR TRANSPORT ASSOCIATION, 2019. *Jet Fuel Price Monitor*. Montreal, Canada: International Air Transport Association. Available at: https://www.iata.org/publications/economics/fuel-monitor/Pages/index.aspx, archived as: https://perma.cc/4PUX-SRLR.

JAYME, Diego Benegas, 2019. Evaluation of Selected Hybrid-Electric Aircraft Projects. Hamburg: Master Thesis, Department of Automotive and Aeronautical Engineering, University of Applied Science of Hamburg. Available at: http://library.ProfScholz.de.

JOHANNING, Andreas, 2017. *Methodik zur Ökobilanzierung im Flugzeugvorentwurf*. München : Verlag Dr. Hut, 2017. Available at: https://www.fzt.haw-hamburg.de/pers/Scholz/Airport2030.html, archived as: http://d-nb.info/1133261876/34.

KERHO, Michael, KRAMER, Brian, 2013. *Turboelectric Distributed Propulsion Test Bed Aircraft*. In: Technical Seminar, FY12 LEARN Phase, 2013. NASA Aeronautics Research Mission Directorate (ARMD). Available at: https://www.nari.arc.nasa.gov/sites/default/files/KERHO_LEARN.pdf, archived as: https://perma.cc/H3JC-YZUS.

KOPPE, Matthias, 2012. *Kraftstoffverbräuche von Turbofan, Propfan und Turboprop im Vergleich. Hamburg: University of Applied Sciences, Hamburg*. Pp 55-62. Available at: http://library.ProfScholz.de, archived as: https://perma.cc/X76Z-TDSY.

KUDELA, Henryk, 2001. Hydraulic losses in pipes. Poland: Wroclaw University of Science. Available at: http://www.energiazero.org/esercizi/hydraulic%20losses%20in%20pipes.pdf, archived as: https://perma.cc/B4LJ-TQGH

LUPELLI, Leonardo, 2011. *A Study on the Integration of the IP Power Offtake system within the Trent 1000 turbofan engine*. Pisa, Italy: Facolta Di Ingegneria, Univeversita Di Pisa. Available at: https://core.ac.uk/download/pdf/14703878.pdf, archived as: https://perma.cc/EHX8-HE4S.

MANOLOPOULOS, Charalampos, LACCHETTI, Matteo, SMITH, Alexander et al., 2018. *Design of Superconducting AC Propulsion Motors for Hybrid Electric Aerospace*. American Institute of Aeronautics and Astronautics 2018-5000. Available at: https://doi.org/10.2514/6.2018-5000.

MEIER, Nathan, 2005. *Jet Engine Specification Database*. Available at: https://www.jet-engine.net, archived as: https://perma.cc/6MBK-S3LT.

NATIONAL ACADEMICS OF SCIENCES, ENGINEERING, AND MEDICINE, 2016. *Commercial Aircraft Propulsion and Energy Systems Research – Reducing Global Carbon Emission*. Washington, DC: The National Academies Press. Pp. 51-59 Available at: http://doi.org/10.17226/23490

NATIONAL PROGRAMME on TECHNOLOGY ENHANCED LEARNING, 2013. *Introduction to Hydraulic Systems.* Guwahati, India: Indian Institute of Technology. P.2 Available at: https://nptel.ac.in/courses/112103174/21, archived as: https://perma.cc/7RRX-HPRM.

NITA, Mihaela Florentina, 2008. *Aircraft Design Studies Based on the ATR 72*. Hamburg: Project, Department of Automotive and Aeronautical Engineering, University of Applied Science of Hamburg. Available at: https://www.fzt.haw-hamburg.de/pers/Scholz/arbeiten/TextNita.pdf, archived as: https://perma.cc/XVT4-6ZHV .

NITA, Mihaela Florentina, 2013. *Contributions to Aircraft Preliminary Design and Optimization*. Hamburg: Dissertation, Department of Automotive and Aeronautical Engineering, University of Applied Science Hamburg. Available at: https://bit.ly/2RmZWL2, archived as: https://perma.cc/2KKA-EBHH.

PARKER AEROSPACE, 2009. Engine-Driven Pumps. Michigan, USA: Parker Hannifin Corporation. Available at: https://prker.co/31Gy7RY, archived as: https://perma.cc/5CFR-NCJE.

PARKER HANNFIN COPORATION, 2013. *Sizing Tube to Maximize System Efficiency*. Ohio, USA. Available at: https://prker.co/2TCx8PN, archived as: https://perma.cc/C74C-8PJ4

PECKNER, Donald, BERNSTEIN, Irving Melvin, 1977. Handbook of Stainless Steels. New York, USA: McGraw-Hill.

PORNET, Clement, 2017. *Conceptual Design methods for Sizing and Performance of Hybrid-Electric Transport Aircraft*. Munich: Technical University of Munich. Pp 66-77. Available at: https://mediatum.ub.tum.de/doc/1399547/1399547.pdf, archived as: https://perma.cc/MV7V-NFWL.

RAPOPORT, Geoff, 2017. *Airbus Pivots Electric Aircraft Plans*. Available at: https://www.avweb.com/recent-updates/business-military/airbus-pivots-electric-aircraft-plans/, archived as: https://perma.cc/R2QA-TPWX

ROSARIO, Ruben Del, 2014. *A Future with Hybrid Electric Propulsion Systems: A NASA Perspective*. In Turbine Engine Technology Symposium Dayton, 2014. Cleveland: NASA Glenn Research Center. Available at: https://ntrs.nasa.gov/archive/nasa/casi.ntrs.nasa.gov/20150000748.pdf, archived as: https://perma.cc/J8BF-Q6WD.

ROSERO, Javier, ORTEGA, Juan, ROMERAL, Luis, 2007. *Moving Towards a More Electric Aircraft*. In: IEEE Aerospace and Systems Magazine, Volume 22, Issue:3, 2007. Available at: https://doi.org/10.1109/MAES.2007.340500.

ROSTEK, Peter, 2015. Electrical Technologies for the Aviation of the Future – Hybrid Electric Propulsion. Tokyo, Japan: Europe-Japan Symposium. Available at: https://sunjet-project.eu/sites/default/files/Airbus%20-%20Delhaye.pdf, archived as: https://perma.cc/F8MK-HZ72.

SCHILTGEN, Benjamin, FREEMAN, Jeffrey, 2016. *Aeropropulsive Interaction and Thermal System Integration within the ECO-150: A Turboelectric Distributed Propulsion Airliner with Conventional Electric Machines*. American Institute of Aeronautics and Astronautics 2016-4064. Available at: https://doi.org/10.2514/6.2016-4064.

SCHOLZ, Dieter, 2014. *Smart Turboprop – A Possible A320 Successor*. In: 4th Symposium on Collaboration in Aircraft Design, Toulouse, France 2014. Aircraft Design and Systems Group, University of Applied Science of Hamburg. Available at: https://www.fzt.haw-hamburg.de/pers/Scholz/Airport2030/Airport2030_PRE_SCAD_14-11-25.pdf, archived as: https://perma.cc/PF2N-N2SM.

SCHOLZ, Dieter, 2018. *Evaluating Aircraft with Electric and Hybrid Propulsion*. In: Electric and Hybrid Aerospace Symposium Cologne, 2018. UKIP Media and Events. Available at: http://doi.org/10.15488/3986.

SCHOLZ, Dieter, 2018a. *Lecture Notes – Aircraft Design*. Hamburg: Hamburg Open Online University (HOOH), University of Applied Science of Hamburg. Available at: http://HOOU.ProfScholz.de

SCHOLZ, Dieter, 2019. *Lecture Notes - Aircraft Systems*. Hamburg: University of Applied Sciences, Hamburg. Available at: https://www.fzt.haw-hamburg.de/pers/Scholz/materialFSs/SkriptNeu.html.

SCHOLZ, Dieter, NITA, Mihaela, 2008. *Method for Preliminary Sizing of Large Propeller Aircraft*. Hamburg: Excel Tool, Department of Automotive and Aeronautical Engineering, University of Applied Science of Hamburg. Available at: https://www.fzt.haw-hamburg.de/pers/Scholz/materialFE/A-C_Preliminary_Sizing_Prop.xls, archived as: https://perma.cc/L2WD-AU7W.

SCHOLZ, Dieter, SERESINHE, Ravinka, STAACK, Ingo, LAWSON, Craig, 2013. *Fuel Consumption Due to Shaft Power Off-Takes from The Engine*. Hamburg: Workshop on Aircraft System Technologies. Available at: https://doi.org/10.15488/4462

SCHWARZE, M.C, 2014. *Superefficient Quiet Short-Range Aircraft*. Stuttgart: Deutscher Luft- und Raumfahrtkongress. Available at: https://pdfs.semanticscholar.org/3fa4/dec5b55458d69ded1f81d1d20229a498c6dd.pdf, archived as: https://perma.cc/T7UY-TWVB.

SKYDROL, 2003. *Technical Bulletin – Type IV Fire Resistant Hydraulic Fluids*. St. Louis, USA: Solutia. Available at: http://skydrol-ld4.com/technical_bulletin_skydrol_4.pdf, archived as: https://perma.cc/SJ5H-DAAS

STÜCKL, Stefan, 2016. Methods for the Design and Evaluation of Future Aircraft Concepts Utilizing Electric Propulsion Systems. Munich: Dissertation, Institute of Aerospace Engineering, Technical University of Munich. Available at: https://d-nb.info/1107543258/34, archived as: https://perma.cc/46XH-XZCY.

TEAL GROUP COPORATION, 2017. *Europrop International TP400*. World Power Systems Briefing. Available at: http://tealgroup.com/images/TGCTOC/sample-wpsba.pdf, archived as: https://perma.cc/M3KQ-72WR.

WARWICK, Graham, 2018. *Europe Eyes Fuel-Saving Boundary-Layer Propulsion*. In: Future of Aerospace. Aviation Week & Space Technology. Available at: https://bit.ly/2mbhDll, archived as: https://perma.cc/PMF3-XLSA.

WELSTEAD, Jason, FELDER, James, 2016. *Conceptual Design of a Single-Aisle Turboelectric Commercial Transport with Fuselage Boundary Layer Ingestion*. In: AIAA SciTech Conference 2016. Hampton, USA: NASA Langley Research Center. Available at: https://ntrs.nasa.gov/search.jsp?R=20160007674.

WELSTEAD, Jason, FELDER, Jim, GUYNN, Mark, et al., 2017. Overview of the NASA STARC-ABL Advanced Concept. Washington, DC, USA: NASA Langley Research Center. Available at : https://ntrs.nasa.gov/search.jsp?R=20170005612.

All links were accessed after 2019-09-22.

Appendix A – Absolute Values of Baseline Aircraft

Table A.1 Aircraft design parameters of A320 and baseline aircraft

	A320	Baseline 1	Baseline 2
Engine Mass (one engine) (kg)	3886.34	3886.34	4001.30
Operating Empty Mass (kg)	41244.00	41244.00	41244.00
Maximum Take-off Mass (kg)	73500.00	72543.55	71038.27
Cruise Speed (m/s)	250.53	237.07	230.19
TSFC/PSFC (kg/N/s / kg/W/s)	1.69E-05	5.50E-08	1.54E-05
Cruise Altitude (ft)	38000.00	29424.66	37808.05
Trip Fuel Mass (kg)	8489.00	7975.39	7703.94
Depreciation Costs ($)	5694769.58	5696220.50	5707755.86
Interest Costs ($)	4686162.61	4687356.56	4696848.88
Insurance Costs ($)	388394.75	388394.74	388394.75
Fuel Costs ($)	3536252.77	3320724.25	3135143.87
Maintenance Costs ($)	6044953.30	6023142.89	6039431.57
Staff Costs ($)	5098062.48	5137475.84	5157989.79
Fees and Charges ($)	10973986.14	10505811.00	9287874.89
DOC (M$)	36.42	35.76	34.41

In Table B.1, the baseline 1 aircraft was based on the all turbo-electric/hydraulic propulsion and baseline 2 aircraft was based on partial turbo-electric hydraulic propulsion.

Appendix B – Absolute Values of TH Aircraft

Table B.1 Aircraft Design Parameters of TSTH2 & TH-16%-Scholz

	TSTH2	TH-16%-Scholz
Engine Mass (one engine) (kg)	3593.04	4289.59
Operating Empty Mass (kg)	44709.76	42050.51
Maximum Take-off Mass (kg)	70952.00	72076.30
Cruise Speed (m/s)	236.88	230.19
TSFC/PSFC (kg/N/s / kg/W/s)	4.99E-08	1.40E-05
Cruise Altitude (ft)	29605.18	37808.05
Trip Fuel Mass (kg)	7891.90	7262.15
Depreciation Costs ($)	5613831.12	5815169.38
Interest Costs ($)	4619559.25	4785238.27
Insurance Costs ($)	382870.77	395989.64
Fuel Costs ($)	3097100.00	2955356.49
Maintenance Costs ($)	5719439.79	6064727.80
Staff Costs ($)	5137203.89	5157989.79
Fees and Charges ($)	10439809.87	9298471.81
DOC (M$)	35.01	34.47

Appendix C - Research Proposal

The original Research Proposal is included on the next pages.

FACHHOCHSCHULE WIENER NEUSTADT
Austrian Network for Higher Education
University of Applied Sciences

ENGINEERING

Research Proposal for a Master Thesis

in Aerospace Engineering

Name of student: Clinton Rodrigo

Autor of Research Proposal: Dieter Scholz

Student registration number: 51819746

Date: 22.01.2019

Table of Contents

I. Working Title

“Basic Comparison of Three Aircraft Concepts: Classic Jet Propulsion, Turbo-Electric Propulsion and Turbo-Hydraulic Propulsion”

Keywords (at least 5): aeronautics, airplanes, aircraft, aircraft design, flight mechanics, aircraft performance, engines, turbofan engines, electric propulsion, hybrid propulsion, hybrid propulsion, distributed propulsion, hydraulics, certification, evaluation, DOC, environment, Airbus, A320

II. Research Question and Task

Research Question:

In light of today's propulsion options for passenger aircraft: What is the superior propulsion principle with respect to Direct Operating Costs and environmental impact? Turbo-electric propulsion, turbo-hydraulic propulsion or the established reference, the turbofan engine?

Task:

- Literature review of electric respectively hybrid propulsion, distributed propulsion as well as the characteristics of turbofan engines, electric engines and hydraulic engines.
- Prepare a very short summary about methods and steps in aircraft design.
- Analyze and compare the three engines in terms of overall aircraft design by integrating them in a short-medium range passenger aircraft using the Preliminary Sizing Tool (PreSTo) for aircraft design based on the Top Level Aircraft Requirements (TLARs) of the Airbus A320 used as reference aircraft in this study. Consider also various option of distributed propulsion for the turbo-electric and turbo-hydraulic concepts.
- Evaluate the three concepts with respect to their fuel burn, Direct Operating Costs (DOC) and environmental impact.
- Discuss your findings and make recommendations based on your results.

III. Research Context

The target to reduce carbon emissions while maintaining the drastic growth in air transport increases the need of improving the existing propulsion systems. With a regular increase in oil price, the operating costs for airlines tend to go up and airlines take the effort to reduce them. Extensive research into advanced propulsion technologies and advanced aircraft configurations can lead to fuel savings, cost reductions and less environmental impact. A sustainable aviation transport system is the final goal. This thesis is a continuation to the work of Prof. Scholz who has worked on the evaluation of electric and hybrid propulsion, aircraft design and simple turbofan models for aircraft design optimization. This thesis is one in a string of student contributions to evaluate new propulsion concepts in aircraft design.

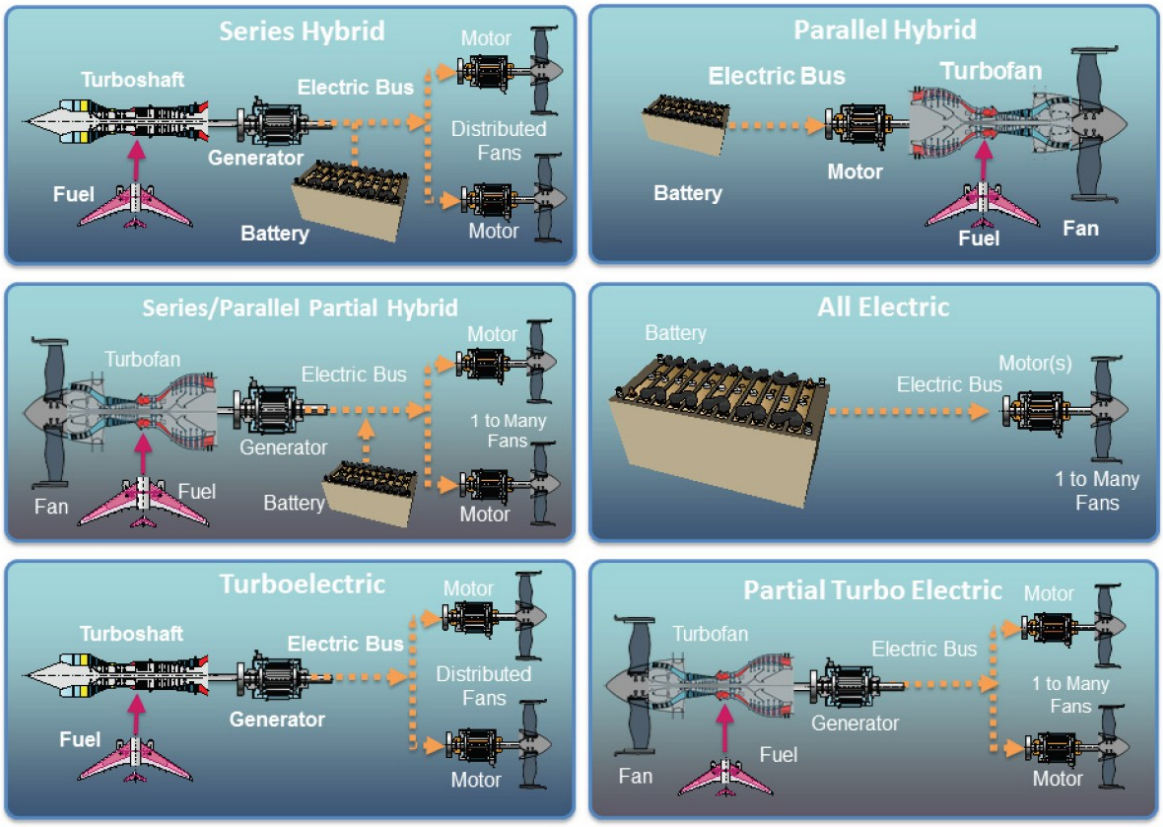

Figure 6 Different hybrid and turbo-electric engine concepts (NAS 2016)

The turbo-electric concept (Figure 1) seems to lead the discussion about new electric propulsion concepts for passenger aircraft. This is due to the fact that batteries would be too heavy for any reasonable range of passenger aircraft – now and in the future. After all, the specific energy (measured in Wh/kg) of kerosene is orders of magnitude higher than that of batteries and hydraulic accumulators.

A hybrid electric system only attenuates the problem of the heavy batteries, but does not solve it. As can easily be seen, a turbo-electric propulsion concepts will have a mass of the propulsion system three times the reference mass of the turbofan engine. Here a turbo-hydraulic concept may show some mass advantages. Also the partial turbo-electric (or turbo-hydraulic) concept may attenuate the problem, but again, is only a blend towards the original turbofan engine.

In a turbo-electric respectively turbo-hydraulic concepts, the energy generated by the gas turbine engine is converted by a generator or a pump into electric current respectively hydraulic volume flow. This energy can be utilized by several fans or propellers that are driven by an electric motor respectively a hydraulic motor. The separation between power generation and thrust generation is called distributed propulsion and is said to bring advantages to the overall system design.

Simple models for engine mass, price and energy efficiency are required for the electric and hydraulic machines. The thesis will contribute to these models with a literature review. The models can then be used in the tested aircraft design environment at the Aircraft Design and Systems Group (AERO) at HAW Hamburg. PreSTo is one aircraft design tool that can be applied. Various methods to calculate the Direct Operating Costs (DOC) for passenger aircraft are in use at AERO. The environmental impact can be calculated with a Life Cycle Analysis (LCA) that was developed especially for evaluations in aircraft design.

IV. Proposed Thesis Outline

Activity	Estimated time *
Performing a literature review	continuously
Studying propulsion system concepts	4 weeks
Defining engine parameters for preliminary sizing and aircraft design	2 weeks
Integrating the propulsion systems into the new aircraft	
Setting up the PreSTo tool for preliminary sizing and aircraft design	4 weeks
Analyzing initial results from the tool to obtain optimum results	
Comparing results from the three propulsion system options	2 weeks
Defining and optimizing possible partial turbo-electric or turbo-hydraulic concepts	4 weeks
Evaluating results from the three propulsion system options. Thesis writing takes place in parallel to all activities.	4 weeks
Discussing results and making recommendations. Finalizing thesis writing.	2 weeks
Total	**22 weeks**

(*) those time estimations are considered as a guideline,

but might be changing during preparation time of the thesis.

V. Advisor

Name : Prof. Dr. Dieter Scholz, MSME
HAW Hamburg (Hochschule für Angewandte Wissenschaften Hamburg)
Department Fahrzeugtechnik und Flugzeugbau
Tel: +49 - 40 - 42875 - 8825 and +49 - 40 - 18 11 98 81 (home office)
E-mail : info@profscholz.de

Name of external supervisor: Prof. Dr.-Ing. Dieter Scholz, MSME

Signature of external supervisor: _____

VI. Literature Sources

NAS 2016

NATIONAL ACADEMIES OF SCIENCES, ENGINEERING, AND MEDICINE: *Commercial Aircraft Propulsion and Energy Systems Research – Reducing Global Carbon Emissions*. Washington, DC : The National Academies Press, 2016. – URL: http://doi.org/10.17226/23490

Scholz 2018a

SCHOLZ, Dieter: *Aircraft Design*. Hamburg Open Online University (HOOU), Hamburg University of Applied Science (HAW Hamburg), Department of Automotive and Aeronautical Engineering, Lecture Notes, 2018. – URL: http://HOOU.ProfScholz.de

Scholz 2018b

SCHOLZ, Dieter: *Evaluating Aircraft with Electric and Hybrid Propulsion*. In: UKIP Media & Events: Conference Proceedings : Electric & Hybrid Aerospace Symposium 2018 (Cologne, 08 -09 November 2018), 2018. – URL: http://doi.org/10.15488/3986 and
URL: https://www.ElectricAndHybridAerospaceTechnology.com

This last reference contains many more suitable references to get started with the thesis. Further help can be found also in http://library.ProfScholz.de. Help on thesis writing (German, English) here: http://ArbeitenHinweise.ProfScholz.de and http://buch.ProfScholz.de (English text on request).